

1 **Chytrid rhizoid morphogenesis is adaptive and resembles hyphal development in**  
2 **'higher' fungi.**

3

4 Davis Laundon<sup>1,2</sup>, Nathan Christmas<sup>1,3</sup>, Glen Wheeler<sup>1</sup> & Michael Cunliffe<sup>1,4</sup>

5

6 <sup>1</sup>Marine Biological Association of the UK, The Laboratory, Citadel Hill, Plymouth, UK

7 <sup>2</sup>School of Environmental Sciences, University of East Anglia, Norwich, UK

8 <sup>3</sup>School of Geographical Sciences, University of Bristol, Bristol, UK

9 <sup>4</sup>School of Biological and Marine Sciences, University of Plymouth, Plymouth, UK

10

11 Correspondence: Michael Cunliffe

12 Marine Biological Association of the United Kingdom,

13 The Laboratory, Citadel Hill, Plymouth, PL1 2PB, UK.

14 E: micnli@mba.ac.uk

15 T: +44 (0)1752 426328

16

17

18

19

20

21

22

23 **Abstract**

24 Fungi are major components of the Earth's biosphere [1], sustaining many critical ecosystem  
25 processes [2, 3]. Key to fungal prominence is their characteristic cell biology, our  
26 understanding of which has been principally based on 'higher' dikaryan hyphal and yeast  
27 forms [4-6]. The early-diverging Chytridiomycota (chytrids) are ecologically important [2, 7, 8]  
28 and a significant component of fungal diversity [9-11], yet their cell biology remains poorly  
29 understood. Unlike dikaryan hyphae, chytrids typically attach to substrates and feed  
30 osmotrophically via anucleate rhizoids [12]. The evolution of fungal hyphae appears to have  
31 occurred from lineages exhibiting rhizoidal growth [13] and it has been hypothesised that a  
32 rhizoid-like structure was the precursor to multicellular hyphae and mycelial feeding in fungi  
33 [14]. Here we show in a unicellular chytrid, *Rhizoclostridium globosum*, that rhizoid  
34 development has equivalent features to dikaryan hyphae and is adaptive to resource  
35 availability. Rhizoid morphogenesis exhibits analogous properties with growth in hyphal  
36 forms, including tip production, branching and decreasing fractal geometry towards the  
37 growing edge, and is controlled by  $\beta$ -glucan-dependent cell wall synthesis and actin  
38 polymerisation. Chytrid rhizoids from individual cells also demonstrate adaptive  
39 morphological plasticity in response to substrate availability, developing a searching  
40 phenotype when carbon starved and exhibiting spatial differentiation when interacting with  
41 particulate substrates. Our results show striking similarities between unicellular early-  
42 diverging and dikaryan fungi, providing insights into chytrid cell biology, ecological  
43 prevalence and fungal evolution. We demonstrate that the sophisticated cell biology and  
44 developmental plasticity previously considered characteristic of hyphal fungi are shared  
45 more widely across the Kingdom Fungi and therefore could be conserved from their most  
46 recent common ancestor.

47

48

## 49 Introduction

50 The phylum Chytridiomycota (chytrids) diverged approximately 750 million years ago and,  
51 with the Blastocladiomycota, formed a critical evolutionary transition in the Kingdom Fungi  
52 dedicated to osmotrophy and the establishment of the chitin-containing cell wall [10]. 407-  
53 million-year-old chytrid fossils from the Devonian Rhynie Chert deposit show chytrids  
54 physically interacting with substrates via rhizoids in a comparative way to extant taxa [15].  
55 Rhizoids play key roles in chytrid ecological function, in terms of both attachment to  
56 substrates and osmotrophic feeding [10, 12]. Yet surprisingly, given the importance of  
57 rhizoids in chytrid ecology, there remains a lack of understanding of chytrid rhizoid biology,  
58 including potential similarities with the functionally analogous hyphae in other fungi.

59 While both rhizoids and hyphae are polar, elongated and bifurcating structures,  
60 rhizoid feeding structures are a basal condition within the true fungi (Eumycota), and the  
61 dikaryan mycelium composed of multicellular septate hyphae is highly derived (Figure 1A  
62 and B). Hyphal cell types are observed outside of the Eumycota, such as within the  
63 Oomycota, however the origin of fungal hyphae within the Eumycota was independent [13,  
64 16] and has not been reported in their closest relatives the Holozoans (animals,  
65 choanoflagellates and their kin). Comparative genomics has indicated that hyphae originated  
66 within the Chytridiomycota-Blastocladiomycota-Zoopagomycota nodes of the fungal tree  
67 [16], and is supported by fossil Blastocladiomycota and extant Monoblepharidomycetes  
68 having hyphae [13, 17]. However, even though rhizoids have been considered precursory to  
69 hyphae [14], comparisons between rhizoid and hyphal developmental biology have not yet  
70 been made.

71 *R. globosum* JEL800 is a monocentric eucarpic chytrid, with extensive anucleate thin  
72 rhizoids ( $230.51 \pm 62.40$  nm in width; Supplementary Figures 1 and 2) and an archetypal  
73 chytrid lifecycle (Figure 1C). With an available sequenced genome [18], easy laboratory  
74 culture and amenability to live cell imaging (this study), *R. globosum* represents a promising  
75 new model organism to investigate the cell biology of rhizoid-bearing, early-diverging fungi.  
76 To study the developing rhizoid system for morphometric analyses, we established a live cell

77 3D/4D confocal microscopy approach in combination with neuron tracing software to 3D  
78 reconstruct developing cells (Figure 1D; Supplementary Figures 3 and 4). From these  
79 reconstructions, we were able to generate a series of cell morphometrics adapted from  
80 neuronal biology to describe and quantify rhizoid development (Supplementary Figure 5).

81

## 82 **Results and Discussion**

### 83 **Chytrid rhizoid morphogenesis fundamentally resembles mycelial development**

84 During rhizoid development we observed a continuous increase in rhizoid length ( $110.8 \pm$   
85  $24.4 \mu\text{m h}^{-1}$ ) ( $n = 5$ ,  $\pm$  SD) and the number of rhizoid tips ( $4.6 \pm 1.2 \text{ tips h}^{-1}$ ) (Figure 1E;  
86 Supplementary Table 1; Supplementary Movies 1-5), with a continuous increase in the  
87 thallus surface area ( $21.1 \pm 5.2 \mu\text{m}^2 \text{ h}^{-1}$ ), rhizoid bifurcations ( $4.2 \pm 1.0 \text{ bifurcations h}^{-1}$ ),  
88 cover area ( $2,235 \pm 170.8 \mu\text{m}^2 \text{ h}^{-1}$ ) and maximum Euclidean distance ( $5.4 \pm 0.1 \mu\text{m h}^{-1}$ )  
89 (Supplementary Figure 6). The rhizoidal growth unit (RGU) (i.e. the distance between two  
90 rhizoid compartments) increased continuously during the first 6 h of the development period  
91 (i.e. cells became relatively less branched) before stabilising during the later phase of growth  
92 (Figure 1E).

93 The RGU patterns that we report here for a unicellular non-hyphal fungus are  
94 comparable to the hyphal growth units (HGU) recorded in multicellular hyphal fungi  
95 (Supplementary Figure 7) [19]. Trinci (1974) assessed hyphal development in three major  
96 fungal lineages (Ascomycota, Basidiomycota, Mucoromycota) and observed that the growth  
97 patterns of major morphometric traits (HGU, total length and number of tips) were similar  
98 across the studied taxa. When the data from our study are directly compared to that of Trinci  
99 (1974), we see that the hyphal growth pattern is also analogous to the rhizoids of the early-  
100 diverging unicellular Chytridiomycota (Supplementary Figure 7).

101 In *R. globosum*, the local rhizoid bifurcation angle remained consistent at  $81.4^\circ \pm 6.3$   
102 after  $\sim 2$  h (Supplementary Figure 6), suggesting the presence of a currently unknown control  
103 mechanism regulating rhizoid branching in chytrids. During rhizoid development, lateral  
104 branching was more frequent than apical branching (Figure 1F and G), as observed in

105 dikaryan hyphae [20]. Fractal analysis (fractal dimension =  $D_b$ ) of 24 h chytrid cells revealed  
106 that rhizoids approximate a 2D biological fractal (Mean  $D_b = 1.51 \pm 0.24$ ), with rhizoids  
107 relatively more fractal at the centre of the cell (Max  $D_b = 1.69$ - $2.19$ ) and less fractal towards  
108 the growing periphery (Min  $D_b = 0.69$ - $1.49$ ) (Supplementary Figure 8). Similar patterns of  
109 fractal organisation are also observed in hyphae-based mycelial colonies [21]. Together  
110 these findings suggest that a form of apical dominance at the growing edge rhizoid tips may  
111 suppress apical branching to maintain rhizoid network integrity as in dikaryan hyphae [22,  
112 23].

113

#### 114 **Cell wall and actin dynamics govern branching in chytrid rhizoids**

115 Given the apparent hyphal-like properties of the chytrid cell, we sought a greater  
116 understanding of the potential subcellular machinery underpinning rhizoid morphogenesis.  
117 Chemical characterisation of the *R. globosum* rhizoid showed that the chitin-containing cell  
118 wall and actin patches were located throughout the rhizoid (Figure 2A). As the cell wall and  
119 actin control hyphal morphogenesis in dikaryan fungi [4-6], they were selected as targets for  
120 chemical inhibition in the chytrid. Inhibition of cell wall  $\beta$ -1,3-glucan synthesis and actin  
121 proliferation with caspofungin and cytochalasin B respectively induced a concentration-  
122 dependent decrease in the RGU and the development of atypical cells with hyperbranched  
123 rhizoids (Figures 2B-D; Supplementary Table 2; Supplementary Movies 6-7). These effects  
124 in *R. globosum* are similar to disruption of normal hyphal branching reported in *Aspergillus*  
125 *fumigatus* (Ascomycota) in the presence of caspofungin [24], and in *Neurospora crassa*  
126 (Ascomycota) in the presence of cytochalasins [25], suggesting that  $\beta$ -1,3-glucan-dependent  
127 cell wall synthesis and actin dynamics also govern branching in chytrid rhizoids by  
128 comparable processes.

129 *In silico* studies of fungal genomes have proposed that the Chytridiomycota  
130 (represented by *Batrachochytrium dendrobatidis*) lack  $\beta$ -1,3-glucan synthase FSK1 gene  
131 homologs [26-28], which is the target for caspofungin. Despite the absence of FKS1  
132 homologues in chytrid genomes, quantification of glucans in *R. globosum* showed that they

133 are present (Figure 2E), with  $58.3 \pm 7.6$  %  $\beta$ -glucans and  $41.6 \pm 7.6$  %  $\alpha$ -glucans of total  
134 glucans.

135 To identify putative  $\beta$ -glucan synthesis genes, we surveyed the *R. globosum* JEL800  
136 genome and focused on glycosyltransferase family 2 (GT2) encoding genes, which include  
137 typical glucan synthases in fungi. A total of 28 GT2 domains were found within 27 genes  
138 (Figure 2F). Of these genes, 20 contained putative chitin synthase domains and many  
139 contained additional domains involved in transcriptional regulation. Nine encode chitin  
140 synthase 2 family proteins and 11 encode chitin synthase 1 family proteins (with two GT2  
141 domains in ORY48846). No obvious genes for  $\beta$ -1,3-glucan or  $\beta$ -1,6-glucan synthases were  
142 found within the genome, consistent with previous *B. dendrobatidis* studies [27, 28].  
143 However, the chitin synthase 2 gene ORY39038 included a putative SKN1 domain (Figure  
144 2F), which has been implicated in  $\beta$ -1,6-glucan synthesis in the ascomycete yeasts  
145 *Saccharomyces cerevisiae* [29] and *Candida albicans* [30]. These results indicate a yet  
146 uncharacterised  $\beta$ -glucan-dependent cell wall production process in chytrids (also targeted  
147 by caspofungin) that is not currently apparent using gene/genome level assessment and  
148 warrants further study.

149

### 150 **Chytrid rhizoids undergo adaptive development in response to carbon starvation**

151 To examine whether chytrids are capable of modifying rhizoid development in response to  
152 changes in resource availability, we exposed *R. globosum* to carbon starvation (i.e.  
153 development in the absence of exogenous carbon). When provided with 10 mM *N*-acetyl-D-  
154 glucosamine (NAG) as an exogenous carbon source, the entire life cycle from zoospore to  
155 sporulation was completed (Supplementary Movie 8). Carbon-starved cells did not produce  
156 zoospores and cell growth stopped after 14-16 h (Supplementary Movie 9). However, using  
157 only endogenous carbon (i.e. zoospore storage lipids) carbon starved cells underwent  
158 substantially differential rhizoid development compared to cells from the exogenous carbon  
159 replete conditions that we interpret to be an adaptive searching phenotype (Figure 3A and B;  
160 Supplementary Table 4; Supplementary Movie 10). Under carbon starvation, *R. globosum*

161 cells invested less in thallus growth than in carbon replete conditions, with the development  
162 of longer rhizoids with a greater maximum Euclidean distance (Figure 3C). Carbon starved  
163 cells were also less branched, had wider bifurcation angles and subsequently covered a  
164 larger surface area. These morphological changes in response to exogenous carbon  
165 starvation (summarised in Figure 3B) suggest that individual chytrid cells are capable of  
166 controlled reallocation of resources away from reproduction (i.e. the production of the  
167 zoosporangium) and towards an extended modified rhizoidal structure indicative of a  
168 resource searching phenotype. Exogenous carbon starvation has also been shown to be  
169 associated with a decrease in branching in the multicellular dikaryan fungus *Aspergillus*  
170 *oryzae* (Ascomycota) [31]. Branching zones in dikaryan mycelia are known to improve  
171 colonisation of trophic substrates and feeding, while more linear 'exploring' zones search for  
172 new resources [32].

173

#### 174 **Chytrids exhibit spatially differentiated rhizoids in response to patchy environments**

175 In the natural environment, chytrids inhabit structurally complex niches made up of  
176 heterologous substrates, such as algal cells [33], amphibian epidermises [34] and  
177 recalcitrant particulate organic carbon [35]. *R. globosum* is a freshwater saprotrophic chytrid  
178 that is typically associated with chitin-rich insect exuviae [36]. We therefore quantified rhizoid  
179 growth of single cells growing on chitin microbeads as an experimental particulate substrate  
180 (Figure 4A and B; Supplementary Movie 11). Initially, rhizoids grew along the outer surface  
181 of the bead and were probably used primarily for anchorage to the substrate. Scanning  
182 electron microscopy (SEM) showed that the rhizoids growing externally on the chitin particle  
183 formed grooves on the bead parallel to the rhizoid axis (Supplementary Figure 1F and G),  
184 suggesting extracellular enzymatic chitin degradation by the rhizoid on the outer surface.  
185 Penetration of the bead occurred during the later stages of particle colonisation (Figure 4A;  
186 Supplementary Movie 12). Branching inside the bead emanated from 'pioneer' rhizoids that  
187 penetrated into the particle (Figure 4C).

188           Given the previous results of the searching rhizoid development in response to  
189 carbon starvation, we created a patchy resource environment using the chitin microbeads  
190 randomly distributed around individual developing cells in otherwise carbon-free media to  
191 investigate how encountering a carbon source affected rhizoid morphology (Figure 4D;  
192 Supplementary Movies 13-15). Particle-associated rhizoids were shorter than rhizoids not in  
193 particle contact, were more branched (i.e. lower RGU), had a shorter maximum Euclidean  
194 distance and covered a smaller area (Figure 4E). These simultaneous feeding and searching  
195 modifications in individual cells linked to particle-associated and non-associated rhizoids  
196 respectively are similar to the rhizoid morphometrics of the cells grown under carbon replete  
197 and carbon deplete conditions previously discussed (Figure 4F and Figure 3B). The  
198 simultaneous display of both rhizoid types in the same cell suggests a controlled spatial  
199 regulation of branching and differentiation of labour within the individual anucleate rhizoidal  
200 network. Functional division of labour is seen in multicellular mycelia fungi [32, 37], including  
201 developing specialised branching structures for increased surface area and nutrient uptake  
202 as in the plant symbiont mycorrhiza (Glomeromycota) [38]. Our observation of similar  
203 complex development in a unicellular chytrid suggests that multicellularity is not a  
204 prerequisite for adaptive spatial differentiation in fungi.

205

## 206 **Conclusions**

207 Appreciation for the ecological significance of chytrids as saprotrophs, parasites and  
208 pathogens is greatly expanding. For example, chytrids are well-established plankton  
209 parasites [8], responsible for the global-scale amphibian pandemic [7] and have recently  
210 emerged as important components of the marine mycobiome [2]. The improved  
211 understanding of chytrid rhizoid biology related to substrate attachment and feeding we  
212 present here opens the door to a greater insight into the functional ecology of chytrids and  
213 their ecological potency. From an evolutionary perspective, the early-diverging fungi are a  
214 critical component of the eukaryotic tree of life [9, 39], including an origin of multicellularity  
215 and the establishment of the archetypal fungal hyphal form, which is responsible in part, for



216 the subsequent colonisation of land by fungi, diversity expansion and interaction with plants  
217 [10]. Our cell biology focused approach advances this developing paradigm by showing that  
218 a representative monocentric, rhizoid-bearing (i.e. non-hyphal) chytrid displays hyphal-like  
219 morphogenesis, with evidence that the cell structuring mechanisms underpinning chytrid  
220 rhizoid development are equivalent to reciprocal mechanisms in dikaryan fungi. Perhaps our  
221 key discovery is that the anucleate chytrid rhizoid shows considerable developmental  
222 plasticity. *R. globosum* is able to control rhizoid morphogenesis to produce a searching form  
223 in response to carbon starvation and, from an individual cell, is capable of spatial  
224 differentiation in adaptation to patchy substrate availability indicating functional division of  
225 labour. The potential for convergent evolution aside, we conclude by parsimony from the  
226 presence of analogous complex cell developmental features in an extant representative  
227 chytrid and dikaryan fungi that adaptive rhizoids, or rhizoid-like structures, are precursory to  
228 hyphae, and are a shared feature of their most recent common ancestor.

229

## 230 **Methods**

231 **Culture and maintenance.** For routine maintenance, *Rhizoclostridium globosum* JEL800  
232 was grown on PmTG agar [40]. Agar plugs were excised from established cultures using a  
233 sterile scalpel, inverted onto new agar plates and incubated at 22 °C in the dark for 48 h.  
234 Developed zoosporangia were sporulated by covering each plug with 100 µl dH<sub>2</sub>O and  
235 incubating at room temperature for 30 min. The released zoospores were distributed across  
236 the agar surface by tilting, dried for 10 min in a laminar flow hood and incubated as above.  
237 To harvest zoospores for experiments, plates were flooded with 1 ml dH<sub>2</sub>O and the zoospore  
238 suspension passed through a 10 µm cell strainer (pluriSelect) to remove mature thalli.  
239 Zoospore density was quantified using a Sedgewick Raft Counter (Pyser SCGI) and a Leica  
240 DM1000 (10 x objective) with cells fixed in 2% formaldehyde at a dilution of 1:1,000.  
241 Zoospores were diluted to a working density of 6.6 x 10<sup>3</sup> ml<sup>-1</sup> for all experiments. Because  
242 PmTG is a complex medium, all experiments detailed below were conducted in Bold's Basal

243 Medium (BBM) supplemented with 1.89 mM ammonium sulfate and 500  $\mu\text{l.l}^{-1}$  F/2 vitamin  
244 solution [41].

245

246 **General cell imaging.** To visualise the rhizoids, cell plasma membranes were labelled with  
247 8.18  $\mu\text{M}$  FM® 1-43 and imaged using a Zeiss LSM 510 Meta confocal laser scanning  
248 microscope (CLSM) (Carl Zeiss) under a 40 x oil-immersion objective lens, with excitation by  
249 a 488 nm Ar laser and emission at 500-530 nm. Z-stacks were acquired at 1  $\mu\text{m}$  intervals.

250 For Scanning Electron Microscopy (SEM) of rhizoids growing along a 2D surface, culture  
251 dishes were lined with EtOH-sterilised Aclar® disks and filled with 3 ml of BBM with 10 mM  
252 NAG, before inoculation with zoospores and incubation for 24 h at 22 °C. For SEM of cells  
253 growing on chitin beads, dishes were prepared as described below and were also inoculated  
254 and incubated for 24 h. Following incubation, cells were fixed overnight in 2.5%

255 glutaraldehyde and then rinsed twice in 0.1 M cacodylate buffer (pH 7.2). Fixed samples  
256 were dehydrated in a graded alcohol series (30%, 50%, 70%, 90%, 100%) with a 15 min  
257 incubation period between each step. Cells were then dried in a Critical Point Drier (K850,

258 Quorum) and attached to SEM sample stubs using carbon infiltrated tabs prior to Cr sputter-  
259 coating using a sputter coating unit (Q150T, Quorum). Samples were imaged with a Field  
260 Emission Gun Scanning Electron Microscope (JSM-7001F, JEOL) operating at 10 kV. For

261 Transmission Electron Microscopy (TEM), 24 h cells grown in suspension were fixed as  
262 previously described. The samples were secondarily fixed with osmium tetroxide (1%, in  
263 buffer pH 7.2, 0.1M) for 1 h, rinsed, and alcohol dehydrated as above. The alcohol was

264 replaced with agar low viscosity resin through a graded resin series (30%, 50%, 70%, 100%,  
265 100%) with 12 h intervals between each step. Samples were transferred to beam capsules  
266 and placed in an embedding oven at 60 °C overnight to enable resin polymerisation. The

267 resulting blocks were sectioned at 50 nm intervals with an ultramicrotome (Ultracut E, Leica)  
268 using a diatome diamond knife. The sections were stained using a saturated solution of  
269 uranyl acetate (for 15 min) and Reynold's lead citrate (15 min) before being examined using

270 a transmission electron microscope (JEM-1400, JEOL).

271

272 **4D rhizoid development.** Glass bottom dishes ( $n = 5$ ) containing 3 ml BBM with 10 mM  
273 NAG as the available carbon source were inoculated with 500  $\mu$ l zoospore suspension.  
274 Zoospores settled for 1h prior to imaging before z-stacks to 50  $\mu$ m depth were acquired at  
275 30 min time intervals for 10 h at 22 °C. Throughout the imaging duration, an optically clear  
276 film permitting gas exchange covered the dish. Branching was counted manually from  
277 maximum intensity projected z-stacks. To quantify rhizoid fractal dimensions, cells were  
278 grown on glass bottom dishes for 24 h. Due to the large size of the 24 h cells, z-stacks were  
279 stitched together in Fiji [42] from four individual stacks. Stitched stacks ( $n = 5$ ) were  
280 converted to maximum intensity projections, processed into binary masks by default  
281 thresholding and denoised. Local Connected Fractal Dimension (LCFD) analysis was  
282 conducted using default parameters on binary masks with the Fiji plugin FracLac [43].

283

284 **Rhizoid tracing and reconstruction.** Z-stacks of rhizoids were imported into the neuron  
285 reconstruction software NeuronStudio [44, 45] and adjusted for brightness and contrast.  
286 Rhizoids were semi-automatically traced with the 'Build Neurite' function using the basal  
287 point of the sporangium as the rhizoidal origin. Tracing used fixed intensity thresholds input  
288 optimally for each image and rhizoids were manually curated and corrected by removing  
289 tracing artefacts (e.g. correcting for loop-splitting). Cells were discarded during quality  
290 control if the tracing was substandard, accounting for the occasional variation in sample size.  
291 Cells grown for 24 h in BBM 10 mM NAG or on chitin beads were too dense to be manually  
292 curated and therefore were automatically traced using dynamic thresholding with a minimum  
293 neurite length of 2  $\mu$ m, although due to their high-density tracings should be considered  
294 imperfect. For 4D image stacks, the rhizoid was reconstructed in 3D at each 30 min interval.  
295 For particle associated and non-associated rhizoids, traced rhizoid systems from individual  
296 cells were manually split into their respective categories.

297 Rhizoids were exported as SWC file extensions [46] and morphometrically quantified  
298 using the btmorph2 library [47] run with Python 3.6.5 implemented in Jupyter Notebook

299 4.4.0. Reconstructed rhizoids were visualised by converting the SWC files first to VTK files  
300 using the swc2vtk Python script (Daisuke Miyamoto: [github.com/ DaisukeMiyamoto](https://github.com/DaisukeMiyamoto/swc2vtk)  
301 [/swc2vtk/](https://github.com/DaisukeMiyamoto/swc2vtk)) and then to OBJ files using the 'Extract Surface' filter in ParaView [48]. OBJ files  
302 were then imported into Blender (2.79), smoothed using automatic default parameters and  
303 rendered for display. OBJ meshes were used for final display only and not analysis. To  
304 visualise chitin beads, z-stacks were imported into the Fiji plugin TrakEM2 [49]. Chitin beads  
305 were manually segmented, and 3D reconstructed by automatically merging traced features  
306 along the z-axis. Meshes were then preliminarily smoothed in TrakEM2 and exported as  
307 OBJ files into Blender for visualisation.

308

309 **Chemical characterisation of the rhizoid.** To label the cell wall and F-actin throughout the  
310 rhizoid system, cells were grown for 24 h in 3 ml BBM with 10 mM NAG on glass bottom  
311 dishes. The culture medium was aspirated from the cells, which were then washed three  
312 times in 500  $\mu$ l 1 x PBS (phosphate buffered saline). Cells were subsequently fixed for 1 h in  
313 4% formaldehyde in 1 x PBS and then washed three times in 1 x PBS and once in PEM (100  
314 mM PIPES (piperazine-N,N'-bis(2-ethanesulfonic acid)) buffer at pH 6.9, 1 mM EGTA  
315 (ethylene glycol tetraacetic acid), and 0.1 mM MgSO<sub>4</sub>). Fixed cells were stained with 1:50  
316 rhodamine phalloidin in PEM for 30 min, washed three times in PEM, and finally stained with  
317 5  $\mu$ g/ml Texas Red-conjugated wheat germ agglutinin (WGA) in PEM for 30 min. Stained  
318 cells were further washed three times in PEM and mounted under a glass coverslip with one  
319 drop of ProLong™ Gold Antifade Mountant (ThermoFisher). Cells were imaged using the  
320 same CLSM as described above with a 63 x oil immersion objective lens. F-Actin was  
321 imaged by excitation with a 543 nm HeNe laser and emission at 535-590 nm, and the cell  
322 wall by excitation with a 633 nm HeNe laser and emission at 650-710 nm. No dye controls  
323 were run for each excitation/emission channel.

324

325 **Chemical inhibition of rhizoid growth.** Autoclaved glass coverslips (VWR) were placed in  
326 a culture dish and submerged in 3 ml BBM with 10 mM NAG. Following 1 h of incubation to

327 allow normal zoospore settlement and germination, 1 ml of growth medium was removed  
328 from the dish and 1 ml of poison-containing media was introduced. Caspofungin diacetate  
329 (working concentration 1-50  $\mu$ M) was used to inhibit cell wall  $\beta$ -glucan synthesis and  
330 cytochalasin B (working concentration 0.1-10  $\mu$ M) was used to inhibit actin filament  
331 formation. Cells were further incubated for 6 h, which was found to be sufficient to observe  
332 phenotypic variation before being removed from the incubator and held at 4 °C prior to  
333 imaging. Coverslips were removed from the dishes using EtOH-cleaned forceps and placed  
334 cell-side down into a glass bottom dish containing 100  $\mu$ l of membrane dye. 3D, as opposed  
335 to 4D imaging, was chosen to allow more replication for statistical analysis. Three plates  
336 were imaged in triplicate ( $n = 9$ ) for each poison treatment and for solvent-only (i.e. no  
337 poison) controls.

338

339  **$\beta$ -glucan quantification.** *R. globosum* was grown to 250 ml in BBM with 10 mM NAG ( $n =$   
340 5) for 7 d before harvesting by centrifugation at 4,700 rpm for 10 min in 50 ml aliquots and  
341 washed in 50 ml MilliQ H<sub>2</sub>O. The cell pellet from each flask was processed for  $\beta$ -glucans in  
342 duplicate using a commercial  $\beta$ -Glucan assay (Yeast & Mushroom) (K-YBGL, Megazyme)  
343 following the manufacturer's protocol. A sample of shop-bought baker's yeast was used as a  
344 control. Glucans were quantified spectrophotometrically using a CLARIOstar® Plus  
345 microplate reader (BMG Labtech).

346

347 **Identification of putative glucan synthases genes.** All glycosyl transferase group 2 (GT2)  
348 domain-containing proteins within the *R. globosum* genome were identified using the JGI  
349 MycoCosm online portal. GT2 functional domains were identified using DELTA-BLAST [50]  
350 and aligned with MAFFT [51]. Maximum Likelihood phylogenies were calculated with RAXML  
351 [52] using the BLOSUM62 matrix and 100 bootstrap replicates and viewed in FigTree  
352 (Andrew Rambaut: [github.com/rambaut/figtree/](https://github.com/rambaut/figtree/)). Overall protein architecture was displayed  
353 using genoplots [53].

354

355 **Carbon starvation and growth on chitin beads.** To quantify differential rhizoidal growth  
356 under carbon replete and carbon deplete conditions, coverslips were placed in a culture dish  
357 and submerged in 3 ml growth medium (either carbon-free BBM or BBM with 10 mM NAG).  
358 Dishes were then inoculated with zoospores and incubated for either 1, 4, 7 or 24 h, with the  
359 24 h cell z-stacks stitched as described in the fractal analysis. Three plates were also  
360 imaged in triplicate for each treatment at each time point ( $n = 9$ ). For both sets of  
361 experiments, cells were imaged as per the chemical inhibition experiments above.

362 Chitin beads (New England Biolabs) were washed three times in carbon-free BBM  
363 using a magnetic Eppendorf rack and suspended in carbon-free BBM at a working  
364 concentration of 1:1,000 stock concentration. Glass bottom dishes containing 3 ml of the  
365 diluted beads were inoculated with zoospores and incubated for either 1, 4, 7 or 24 h prior to  
366 imaging. For imaging, the culture medium was aspirated off and beads were submerged in  
367 100  $\mu$ l FM® 1-43. Three plates were imaged in triplicate for each time point ( $n = 9$ ). To  
368 understand rhizoid development in a starved cell that had encountered a chitin bead, we  
369 imaged cells that contacted a chitin bead following development along the glass bottom of  
370 the dish.

371

372 **Statistical Analysis.** Rhizoid width was measured from TEM images ( $n = 25$ ). The  
373 comparison between apical and lateral branching was conducted using a Wilcoxon Rank  
374 Sum test. Univariate differences in rhizoid morphometrics between experimental treatments  
375 were evaluated using Welch's t-tests unless stated otherwise. Shapiro-Wilk and Levene's  
376 tests were used to assess normality and homogeneity of variance respectively. If these  
377 assumptions could not be met, then Wilcoxon Rank Sum was used as a nonparametric  
378 alternative. Univariate morphometric differences between particle-associated and non-  
379 associated rhizoids were evaluated using a paired t-test. All data were analysed in RStudio  
380 v1.1.456. [54]

381

382 **Data availability**

383 All data that support the findings of this study are freely available via the corresponding  
384 author.

385

### 386 **Acknowledgements**

387 The authors would like to thank Glenn Harper, Alex Strachan and the team at the Plymouth  
388 Electron Microscopy Centre (PEMC) for their assistance. We are indebted to Joyce  
389 Longcore (University of Maine) for providing *R. globosum* JEL800 from her chytrid culture  
390 collection (now curated by the Collection of Zoosporic Eufungi at the University of Michigan).

391

### 392 **Funding**

393 D.L. is supported by an EnvEast Doctoral Training Partnership (DTP) PhD studentship  
394 funded from the UK Natural Environment Research Council (NERC). M.C. is supported by  
395 the European Research Council (ERC) (MYCO-CARB project; ERC grant agreement  
396 number 772584). N.C. is supported by NERC (Marine-DNA project; NERC grant number  
397 NE/N006151/1). G.W. is supported by an MBA Senior Research Fellowship.

398

### 399 **Author Contributions**

400 D.L. and M.C. conceived the study. D.L. conducted the laboratory work and data analysis.  
401 N.C. analysed the *R. globosum* JEL800 genome. G.W. provided support with microscopy.  
402 M.C. secured the funding. D.L. and M.C. critically assessed and interpreted the findings. D.L.  
403 and M.C. wrote the manuscript, with the help of N.C. and G.W.

404

### 405 **Competing Interests**

406 The authors declare no competing interests

407

408 **References**

- 409 1. Bar-On, Y.M., R. Phillips, and R. Milo, *The biomass distribution on Earth*.  
410 Proceedings of the National Academy of Sciences, 2018. **115**(25): p. 6506-6511
- 411 2. Grossart, H.-P., et al., *Fungi in aquatic ecosystems*. Nature Reviews Microbiology,  
412 2019. **17**(6): p. 339-354.
- 413 3. Peay, K.G., P.G. Kennedy, and J.M. Talbot, *Dimensions of biodiversity in the Earth*  
414 *mycobiome*. Nature Reviews Microbiology, 2016. **14**: p. 434.
- 415 4. Riquelme, M., et al., *Fungal Morphogenesis, from the Polarized Growth of Hyphae to*  
416 *Complex Reproduction and Infection Structures*. Microbiology and Molecular Biology  
417 Reviews, 2018. **82**(2): p. e00068-17.
- 418 5. Steinberg, G., et al., *Cell Biology of Hyphal Growth*, in *The Fungal Kingdom*. 2017,  
419 American Society of Microbiology.
- 420 6. Gow, N.A.R., J.-P. Latge, and C.A. Munro, *The Fungal Cell Wall: Structure,*  
421 *Biosynthesis, and Function*. Microbiology Spectrum, 2017. **5**(3).
- 422 7. O'Hanlon, S.J., et al., *Recent Asian origin of chytrid fungi causing global amphibian*  
423 *declines*. Science, 2018. **360**(6389): p. 621-627.
- 424 8. Frenken, T., et al., *Integrating chytrid fungal parasites into plankton ecology:*  
425 *research gaps and needs*. Environmental Microbiology, 2017. **19**(10): p. 3802-3822.
- 426 9. James, T.Y., et al., *Reconstructing the early evolution of Fungi using a six-gene*  
427 *phylogeny*. Nature, 2006. **443**(7113): p. 818-822.
- 428 10. Berbee, M.L., T.Y. James, and C. Strullu-Derrien, *Early diverging fungi: diversity and*  
429 *impact at the dawn of terrestrial life*. Annual Review of Microbiology, 2017. **71**(1): p.  
430 41-60.
- 431 11. Tedersoo, L., et al., *High-level classification of the Fungi and a tool for evolutionary*  
432 *ecological analyses*. Fungal Diversity, 2018. **90**(1): p. 135-159.
- 433 12. Stajich, J.E., et al., *The Fungi*. Current Biology, 2009. **19**(18): p. R840-R845.



- 434 13. Dee, J.M., et al., *Cytology and molecular phylogenetics of Monoblepharidomycetes*  
435 *provide evidence for multiple independent origins of the hyphal habit in the Fungi.*  
436 *Mycologia*, 2015. **107**(4): p. 710-728.
- 437 14. Harris, S.D., *Hyphal morphogenesis: an evolutionary perspective.* *Fungal Biology*,  
438 2011. **115**: p. 475-484.
- 439 15. Strullu-Derrien, C., et al., *A New Chytridiomycete Fungus Intermixed with Crustacean*  
440 *Resting Eggs in a 407-Million-Year-Old Continental Freshwater Environment.* *PLOS*  
441 *ONE*, 2016. **11**(12): p. e0167301.
- 442 16. Kiss, E., et al., *Comparative genomics reveals the origin of fungal hyphae and*  
443 *multicellularity.* *bioRxiv*, 2019: p. 546531.
- 444 17. Strullu-Derrien, C., et al., *New insights into the evolutionary history of Fungi from a*  
445 *407 Ma Blastocladiomycota fossil showing a complex hyphal thallus.* *Philosophical*  
446 *Transactions of the Royal Society B: Biological Sciences*, 2018. **373**(1739): p.  
447 20160502.
- 448 18. Mondo, S.J., et al., *Widespread adenine N6-methylation of active genes in fungi.*  
449 *Nature Genetics*, 2017. **49**: p. 964.
- 450 19. Trinci, A.P.J., *A Study of the Kinetics of Hyphal Extension and Branch Initiation of*  
451 *Fungal Mycelia.* *Microbiology*, 1974. **81**(1): p. 225-236.
- 452 20. Harris, S.D., *Branching of fungal hyphae: regulation, mechanisms and comparison*  
453 *with other branching systems.* *Mycologia*, 2008. **100**(6): p. 823-832.
- 454 21. Obert, M., P. Pfeifer, and M. Sernetz, *Microbial growth patterns described by fractal*  
455 *geometry.* *Journal of Bacteriology*, 1990. **172**(3): p. 1180-1185.
- 456 22. Harris, S.D., *Hyphal branching in filamentous fungi.* *Developmental Biology*, 2019.  
457 **451**(1): p. 35-39.
- 458 23. Semighini, C.P. and S.D. Harris, *Regulation of Apical Dominance in Aspergillus*  
459 *nidulans Hyphae by Reactive Oxygen Species.* *Genetics*, 2008. **179**(4): p. 1919-  
460 1932.

- 461 24. Moreno-Velásquez, S.D., et al., *Caspofungin-mediated growth inhibition and*  
462 *paradoxical growth in Aspergillus fumigatus involve fungicidal hyphal tip lysis coupled*  
463 *with regenerative intrahyphal growth and dynamic changes in  $\beta$ -1,3-glucan synthase*  
464 *localization*. Antimicrobial Agents and Chemotherapy, 2017. **61**(10): p. e00710-17.
- 465 25. Allen, E.D., R. Aiuto, and A.S. Sussman, *Effects of cytochalasins on Neurospora*  
466 *crassa*. Protoplasma, 1980. **102**(1): p. 63-75.
- 467 26. Ruiz-Herrera, J. and L. Ortiz-Castellanos, *Cell wall glucans of fungi. A review*. The  
468 Cell Surface, 2019. **5**: p. 100022.
- 469 27. Richards, T.A., G. Leonard, and J.G. Wideman, *What Defines the "Kingdom" Fungi?*  
470 Microbiology Spectrum, 2017. **5**(3).
- 471 28. Ruiz-Herrera, J. and L. Ortiz-Castellanos, *Analysis of the phylogenetic relationships*  
472 *and evolution of the cell walls from yeasts and fungi*. FEMS Yeast Research, 2010.  
473 **10**(3): p. 225-243.
- 474 29. Roemer, T., S. Delaney, and H. Bussey, *SKN1 and KRE6 define a pair of functional*  
475 *homologs encoding putative membrane proteins involved in beta-glucan synthesis*.  
476 Molecular and Cellular Biology, 1993. **13**(7): p. 4039-4048.
- 477 30. Han, Q., et al., *Blocking  $\beta$ -1,6-glucan synthesis by deleting KRE6 and SKN1*  
478 *attenuates the virulence of Candida albicans*. Molecular Microbiology, 2019. **111**(3):  
479 p. 604-620.
- 480 31. Pollack, J.K., Z.J. Li, and M.R. Marten, *Fungal mycelia show lag time before re-*  
481 *growth on endogenous carbon*. Biotechnology and bioengineering, 2008. **100**(3): p.  
482 458-465.
- 483 32. Vinck, A., et al., *Hyphal differentiation in the exploring mycelium of Aspergillus niger*.  
484 Molecular Microbiology, 2005. **58**(3): p. 693-699.
- 485 33. Canter, H.M. and J.W.G. Lund, *Studies on plankton parasites. I. Fluctuations in*  
486 *numbers of Asterionella formosa Hass. in relation to fungal epidemics*. New  
487 Phytologist, 1948. **47**: p. 238-261.

- 488 34. Longcore, J.E., A.P. Pessier, and D.K. Nichols, *Batrachochytrium dendrobatidis* gen.  
489 *et sp. nov.*, a chytrid pathogenic to amphibians. *Mycologia*, 1999. **91**(2): p. 219-227.
- 490 35. Gleason, F.H., et al., *The ecology of chytrids in aquatic ecosystems: roles in food*  
491 *web dynamics*. *Fungal Biology Reviews*, 2008. **22**(1): p. 17-25.
- 492 36. Sparrow, F.K., *Aquatic Phycomycetes*. 1960, Ann Arbor: The University of Michigan  
493 Press.
- 494 37. Boddy, L., *Saprotrophic Cord-Forming Fungi: Meeting the Challenge of*  
495 *Heterogeneous Environments*. *Mycologia*, 1999. **91**(1): p. 13-32.
- 496 38. Bago, B., et al., *Branched absorbing structures (BAS): a feature of the extraradical*  
497 *mycelium of symbiotic arbuscular mycorrhizal fungi*. *New Phytologist*, 1998. **139**(2):  
498 p. 375-388.
- 499 39. Jones, M.D.M., et al., *Discovery of novel intermediate forms redefines the fungal tree*  
500 *of life*. *Nature*, 2011. **474**: p. 200.
- 501 40. Donald, J.S.B., *Allochytridium expandens Rediscovered: Morphology, Physiology*  
502 *and Zoospore Ultrastructure*. *Mycologia*, 1986. **78**(3): p. 439-448.
- 503 41. Guillard, R.R.L. and J.H. Ryther, *Studies of marine planktonic diatoms. I. Cyclotella*  
504 *nana Hustedt and Detonula confervaceae (Cleve) Gran*. *Canadian Journal of*  
505 *Microbiology*, 1967. **8**: p. 229-239.
- 506 42. Schindelin, J., et al., *Fiji: an open-source platform for biological-image analysis*.  
507 *Nature Methods*, 2012. **9**: p. 676.
- 508 43. Karperien, A., H. Ahammer, and H. Jelinek, *Quantitating the subtleties of microglial*  
509 *morphology with fractal analysis*. *Frontiers in Cellular Neuroscience*, 2013. **7**(3).
- 510 44. Rodriguez, A., et al., *Rayburst sampling, an algorithm for automated three-*  
511 *dimensional shape analysis from laser scanning microscopy images*. *Nature*  
512 *Protocols*, 2006. **1**(4): p. 2152-2161.
- 513 45. Rodriguez, A., et al., *Automated Three-Dimensional Detection and Shape*  
514 *Classification of Dendritic Spines from Fluorescence Microscopy Images*. *PLOS*  
515 *ONE*, 2008. **3**(4): p. e1997.

- 516 46. Stockley, E.W., et al., *A system for quantitative morphological measurement and*  
517 *electrotonic modelling of neurons: three-dimensional reconstruction*. Journal of  
518 Neuroscience Methods, 1993. **47**(1): p. 39-51.
- 519 47. Torben-Nielsen, B., *An Efficient and Extendable Python Library to Analyze Neuronal*  
520 *Morphologies*. Neuroinformatics, 2014. **12**(4): p. 619-622.
- 521 48. Ahrens, J., B. Geveci, and C. Law, *ParaView: An End-User Tool for Large-Data*  
522 *Visualization*, in *Visualization Handbook*, C.D. Hansen and C.R. Johnson, Editors.  
523 2005, Butterworth-Heinemann: Burlington. p. 717-731.
- 524 49. Cardona, A., et al., *TrakEM2 Software for Neural Circuit Reconstruction*. PLOS ONE,  
525 2012. **7**(6): p. e38011.
- 526 50. Boratyn, G.M., et al., *Domain enhanced lookup time accelerated BLAST*. Biology  
527 Direct, 2012. **7**(1): p. 12.
- 528 51. Katoh, K. and D.M. Standley, *MAFFT Multiple Sequence Alignment Software Version*  
529 *7: Improvements in Performance and Usability*. Molecular Biology and Evolution,  
530 2013. **30**(4): p. 772-780.
- 531 52. Stamatakis, A., *RAxML version 8: a tool for phylogenetic analysis and post-analysis*  
532 *of large phylogenies*. Bioinformatics, 2014. **30**(9): p. 1312-1313.
- 533 53. Guy, L., J.R. Kultima, and S.G.E. Andersson, *genoPlotR: comparative gene and*  
534 *genome visualization in R*. Bioinformatics (Oxford, England), 2010. **26**(18): p. 2334-  
535 2335.
- 536 54. R-Studio, T., *RStudio: Integrated Development for R*. 2015, Boston, MA: RStudio,  
537 Inc.
- 538
- 539

540 **Figure Legends**

541 **Figure 1 - Rhizoids are the basal feeding condition within the fungal kingdom and**  
542 **their morphogenesis is similar to hyphal development.** (A-B) Correlating the major  
543 feeding types in fungi (A) to phylogeny (B) shows rhizoids to be the basal feeding condition  
544 in the true fungi (Eumycota). Tree adapted from [11]. (C) *R. globosum* exhibits an archetypal  
545 chytrid lifecycle. (D) Chytrid rhizoids were reconstructed using the neuron tracing workflow  
546 outlined in Supplementary Figure 3. Example of a 3D reconstructed *R. globosum* rhizoid  
547 system taken from a 10 h time series. Scale bar = 20  $\mu\text{m}$ . (E) Rhizoid growth trajectories for  
548 4D confocal time series ( $n = 5$ , mean  $\pm$  S.E.M.) of rhizoidal growth unit, total length and  
549 number of tips. (F) Apical and lateral branches occur in chytrid rhizoids. Apical branching  
550 occurs when a branch is formed at the rhizoid tip parallel to the established rhizoidal axis.  
551 Lateral branching occurs when a branch is formed distally to the rhizoidal tip, establishing a  
552 new rhizoidal axis. (G) 4D confocal imaging ( $n = 5$ , mean  $\pm$  S.E.M.) revealed that lateral  
553 branching dominates over apical branching  $*p < 0.05$ .

554

555 **Figure 2 - Cell wall synthesis and actin dynamics govern rhizoid branching.** (A)  
556 Fluorescent labelling of cell wall and actin structures in 24 h *R. globosum* cells. The cell wall  
557 and actin patches were found throughout the rhizoid. WGA = conjugated Wheat Germ  
558 Agglutinin. Scale bar = 10  $\mu\text{m}$ . (B) Representative 3D reconstructions of 7 h *R. globosum*  
559 cells following treatment with caspofungin diacetate and cytochalasin B at stated  
560 concentrations to inhibit cell wall and actin filament biosynthesis respectively, relative to  
561 solvent only controls. Scale bar = 20  $\mu\text{m}$  (C) Application of caspofungin diacetate and  
562 cytochalasin B resulted in a concentration-dependent decrease in the rhizoidal growth unit,  
563 resulting in atypical hyperbranched rhizoids ( $n \sim 9$ , mean  $\pm$  S.E.M.). n.s  $p > 0.05$  (not  
564 significant),  $*p < 0.05$ ,  $**p < 0.01$ ,  $***p < 0.001$ . This differential growth is diagrammatically  
565 summarised in (D). (E)  $\beta$ -glucan concentration of *R. globosum* ( $n = 10$ ) relative to a baker's  
566 yeast control ( $n = 2$ ). (F) Maximum likelihood phylogeny of GT2 domains (BcsA and WcaA  
567 domains) within the *R. globosum* genome (midpoint rooting). Full architecture of each protein

568 is shown. Asterisk indicates the putative glucan synthesis protein ORY39038 containing a  
569 putative SKN1 domain.

570

571 **Figure 3 - Chytrids are capable of adaptive rhizoid development under carbon**

572 **starvation.** (A) Representative 3D reconstructions of *R. globosum* cells grown under carbon

573 replete or carbon deplete conditions at different timepoints. Scale bar = 20  $\mu\text{m}$ . When

574 exposed to carbon starvation, chytrids are capable of differential adaptive growth to produce

575 a searching phenotype. This differential growth is summarised in (B). (C) Differential growth

576 trajectories of major morphometric traits between *R. globosum* cells ( $n \sim 9$ , mean  $\pm$  S.E.M.)

577 grown under carbon replete and carbon deplete conditions over time. n.s  $p > 0.05$  (not

578 significant), \* $p < 0.05$ , \*\* $p < 0.01$ , \*\*\* $p < 0.001$

579

580 **Figure 4 - Rhizoids associated with heterogenous particulate carbon exhibit spatial**

581 **differentiation** (A) Representative 3D reconstructions of *R. globosum* cells (blue) growing

582 on chitin beads (beige) at different timepoints. Scale bar = 20  $\mu\text{m}$ . (B) Growth trajectories for

583 total rhizoid length and thallus surface area for *R. globosum* cells growing on chitin beads ( $n$

584  $\sim 9$ , mean  $\pm$  S.E.M.). (C) Diagrammatic summary of *R. globosum* rhizoid development on

585 chitin beads. (D) Representative 3D reconstruction of a 24 h searching *R. globosum* cell

586 (blue) that has encountered a chitin bead (beige). The colour coded panel shows parts of the

587 rhizoid system in contact (green) and not in contact (blue) with the bead. Scale bar = 20  $\mu\text{m}$ .

588 (E) Comparison of rhizoids in contact or not in contact with the chitin bead ( $n = 8$ , mean  $\pm$

589 S.E.M.). (F) Diagrammatic summary of spatial differentiation in a starved, searching rhizoid

590 that has encountered a particulate carbon patch.

591

592 **Supplementary Figure 1 - Scanning Electron Microscopy (SEM) images of *R.***

593 ***globosum* rhizoids.** (A-D) *R. globosum* cells grown on a 2D, inert surface (Aclar®) in NAG

594 supplemented media. (A) Shown are multiple thalli anchored to the surface by threadlike

595 rhizoids. (B) The spherical thallus of *R. globosum* is connected to the rhizoid system via an

596 apophysis (subsporangial swelling). (C) High-magnification image of the apophysis. (D)  
597 Rhizoids are branched and bifurcating structures that frequently overlap. The fusion of  
598 rhizoids (anastomoses) was never observed from SEM images. (E-G) Chytrid cells growing  
599 on chitin beads. (F-G) External rhizoids growing along the surface of the particle formed  
600 superficial lacerations (indicated by asterisks). a, apophysis; b, bifurcation; t, thallus. Scale  
601 bar (A,E) = 10  $\mu\text{m}$ . Scale bar (B-D, F-G) = 1  $\mu\text{m}$ .

602

603 **Supplementary Figure 2 - Transmission Electron Microscopy (TEM) images of *R.***

604 ***globosum* rhizoids.** (A-C) TEM images of the apophysis. The apophysis is not septated  
605 from the thallus and the two are connected by continuous cytoplasm (A-B), as are the  
606 apophysis and the rhizoid (C). (D-F) TEM images of the apophysis. The rhizoid is always  
607 enveloped by a cell wall and no structure was observed to demarcate rhizoid branches at  
608 bifurcation nodes (D). Although no formal subcellular organelles could be identified within the  
609 rhizoid, a dense and complex endomembrane system permeated the entire system (E-F).  
610 This suggested that the rhizoid is a dynamic organelle governed by high levels of trafficking  
611 and endomembrane reorganisation. a, apophysis; b, bifurcations; e, endomembrane; r,  
612 rhizoid; w, cell wall. Asterisks mark the connection between the apophysis and the thallus.  
613 Scale bar (A) = 2  $\mu\text{m}$ . Scale bar (B-F) = 200 nm.

614

615 **Supplementary Figure 3 - Neuron tracing was used to reconstruct and quantify chytrid**

616 **rhizoid development.** Flow-diagram protocol for the acquisition, reconstruction, analysis  
617 and visualisation of *R. globosum* rhizoids based on neuron tracing.

618

619 **Supplementary Figure 4 - 3D reconstructions of developing *R. globosum* rhizoids.**

620 Total series of 3D reconstructed *R. globosum* rhizoids taken from 4D development  
621 experiments. Scale bar = 20  $\mu\text{m}$ .

622

623 **Supplementary Figure 5 - Chytrid rhizoids were quantified using morphometric**  
624 **parameters adapted from neurobiology.** Diagrammatic glossary of neuronal morphometric  
625 parameters used to describe 3D reconstructed chytrid rhizoids from growth experiments.  
626 Chytrids are represented by an aerial 2D diagram, as if from a z-stack maximum intensity  
627 projection.

628

629 **Supplementary Figure 6 - Development trajectories of major morphometric traits in *R.***  
630 ***globosum* rhizoids.** Growth patterns of morphometric features for developing *R. globosum*  
631 rhizoids taken from 4D microscopy experiments. Plateau in the z-axis depth occurs due  
632 growth outside of the designated experimental imaging field. Scale bar = 20  $\mu\text{m}$ .

633

634 **Supplementary Figure 7 - Development of chytrid rhizoids fundamentally resembles**  
635 **mycelial development in hyphal fungi.** Comparison of the growth trajectories of the growth  
636 unit, total length and number of tips of the rhizoids or hyphae in fungi from the Ascomycota,  
637 Basidiomycota, Mucoromycota and Chytridiomycota. Data for Ascomycota, Basidiomycota  
638 and Mucoromycota fungi are not from this study and are reproduced as new figures directly  
639 from (Trinci, 1974).

640

641 **Supplementary Figure 8 - Fractal organisation of the chytrid rhizoid resembles that of**  
642 **mycelial colonies.** Processing and fractal analysis workflow for 24 h *R. globosum* cells.  
643 Chytrid rhizoid systems become decreasingly fractal towards the growing edge. Final column  
644 images are pseudo-coloured by fractal dimension.

645

646 **Supplementary Table 1 – Morphometric features of developing *R. globosum* rhizoids**  
647 **associated with Figure 1 E-G.**

648

649 **Supplementary Table 2 – Morphometric features and statistical comparisons of**  
650 **chemically inhibited *R. globosum* rhizoids, associated with Figure 2 B-C.**



651

652 **Supplementary Table 3 – Morphometric features and statistical comparisons of *R.***  
653 ***globosum* rhizoids growing in carbon replete or deplete media, associated with Figure**  
654 **3 A-C.**

655

656 **Supplementary Table 4 – Morphometric features of *R. globosum* rhizoids growing on**  
657 **chitin beads, associated with Figure 4 A-B.**

658

659 **Supplementary Table 5 – Morphometric features and statistical comparisons of**  
660 **searching *R. globosum* rhizoids encountering chitin beads, associated with Figure 4**  
661 **D-E.**

662

663 **Supplementary Movie 1 – 4D imaging of developing *R. globosum* rhizoids used for**  
664 **quantifying morphometric growth trajectories (Replicate 1). Time in HH:MM**

665

666 **Supplementary Movie 2 – 4D imaging of developing *R. globosum* rhizoids used for**  
667 **quantifying morphometric growth trajectories (Replicate 2). Time in HH:MM**

668

669 **Supplementary Movie 3 – 4D imaging of developing *R. globosum* rhizoids used for**  
670 **quantifying morphometric growth trajectories (Replicate 3). Time in HH:MM**

671

672 **Supplementary Movie 4 – 4D imaging of developing *R. globosum* rhizoids used for**  
673 **quantifying morphometric growth trajectories (Replicate 4). Time in HH:MM**

674

675 **Supplementary Movie 5 – 4D imaging of developing *R. globosum* rhizoids used for**  
676 **quantifying morphometric growth trajectories (Replicate 5). Time in HH:MM**

677

678 **Supplementary Movie 6 – Representative 3D reconstructions of 7 h *R. globosum***  
679 **rhizoids from caspofungin treated and control cells.** Cell wall inhibited rhizoids display  
680 atypical hyperbranching.

681

682 **Supplementary Movie 7 – Representative 3D reconstructions of 7 h *R. globosum***  
683 **rhizoids from cytochalasin B treated and control cells.** Actin inhibited rhizoids display  
684 atypical hyperbranching.

685

686 **Supplementary Movie 8 – 4D imaging of the entire *R. globosum* life cycle growing on**  
687 **10 mM NAG.** Cell completes its entire lifecycle and sporulates. Time in HH:MM

688

689 **Supplementary Movie 9 – 4D imaging of *R. globosum* growing in carbon deplete**  
690 **media.** Cell does not complete lifecycle and ceases growth after 14-16 h. Time in HH:MM

691

692 **Supplementary Movie 10 – Representative 3D reconstructions of *R. globosum***  
693 **rhizoids from carbon replete and carbon deplete cells.** Cells in the carbon deplete  
694 condition display the differential searching phenotype. Reconstructions are scaled relative to  
695 timepoint.

696

697 **Supplementary Movie 11 – Representative 3D reconstructions of *R. globosum***  
698 **rhizoids from cells growing on chitin beads.** Reconstructions are scaled relative to  
699 timepoint.

700

701 **Supplementary Movie 12 – 4D imaging of *R. globosum* growing on a chitin microbead.**  
702 Note that branching within the bead emanates from ‘pioneer’ penetrative rhizoids. Time in  
703 HH:MM

704

705 **Supplementary Movie 13 – 4D imaging of searching *R. globosum* rhizoids**  
706 **encountering a chitin bead (XY).** Note how rhizoids not in contact with the particle continue  
707 to grow in a searching pattern. Time in HH:MM  
708  
709 **Supplementary Movie 14 – 4D imaging of searching *R. globosum* rhizoids**  
710 **encountering a chitin bead (YZ).** Note how branching is most profuse in rhizoids in contact  
711 with the particle. Time in HH:MM  
712  
713 **Supplementary Movie 15 – Representative 3D reconstruction of *R. globosum* rhizoids**  
714 **from a searching cell in carbon deplete media that has encountered a chitin**  
715 **microbead.** The rhizoid is spatially differentiated and coloured whether in contact (green) or  
716 not in contact with (blue) the chitin bead.  
717  
718 **Supplementary File 1 – Total raw data used for analysis in this study**  
719  
720

Figure 1

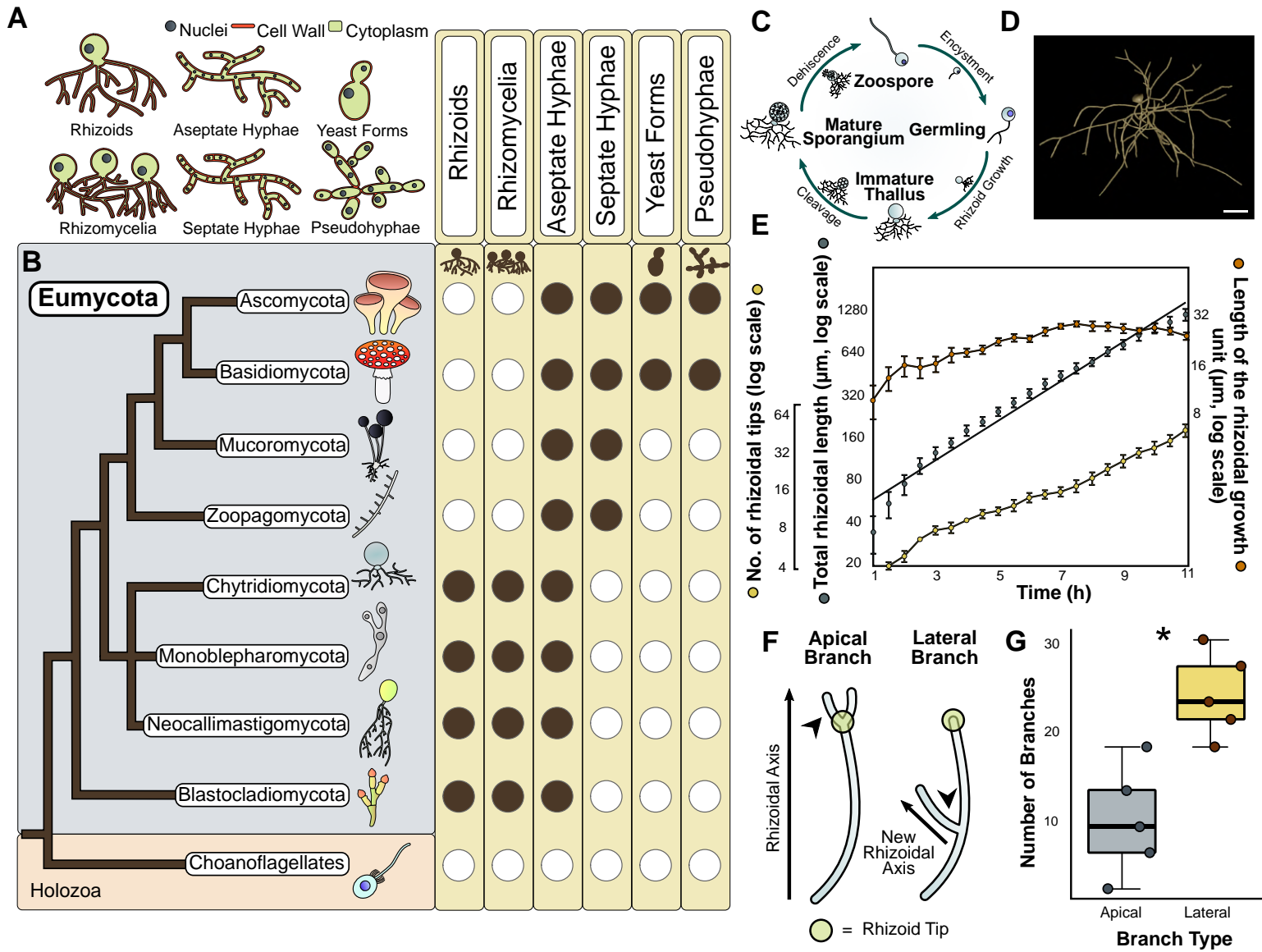


Figure 2

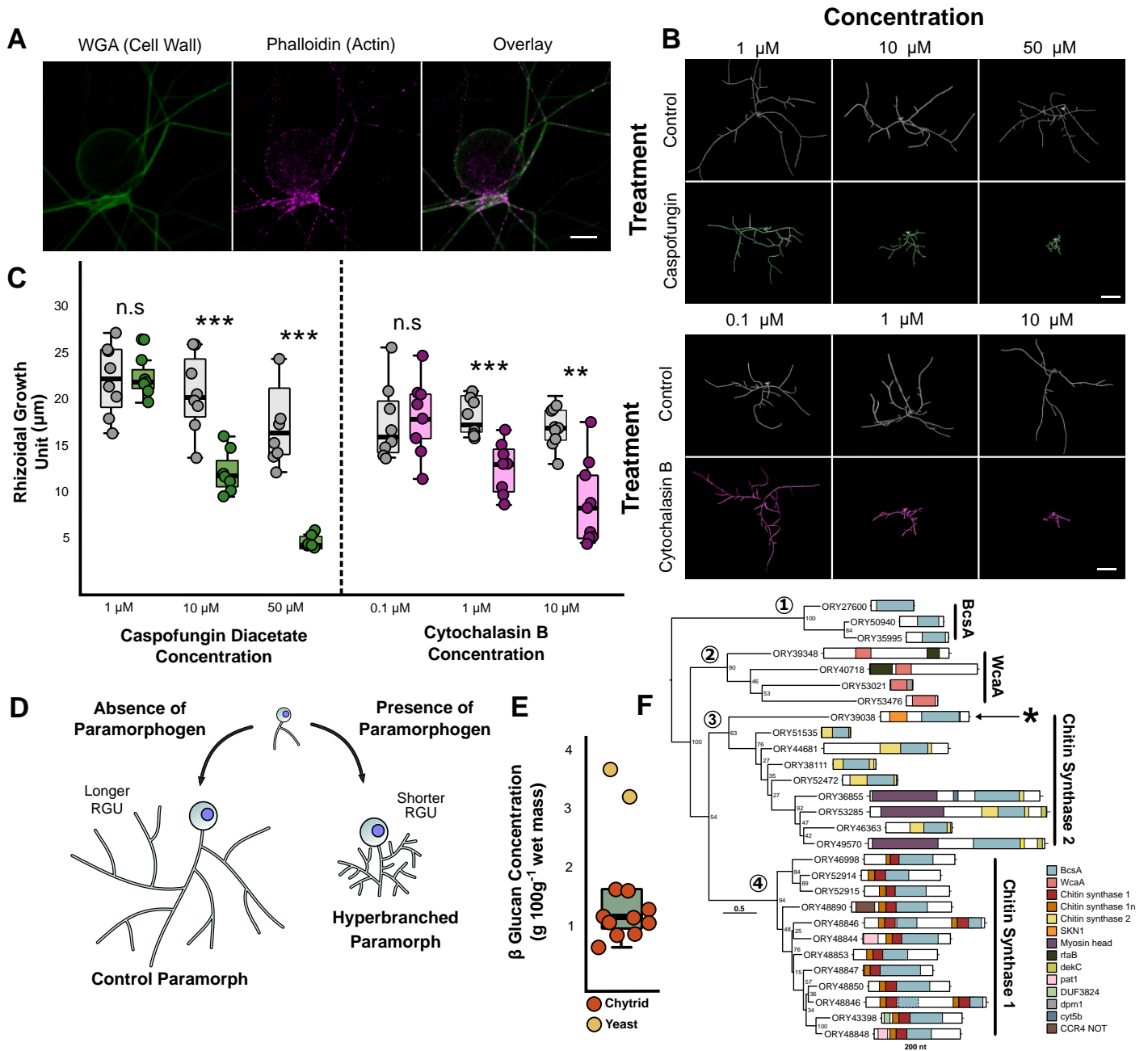
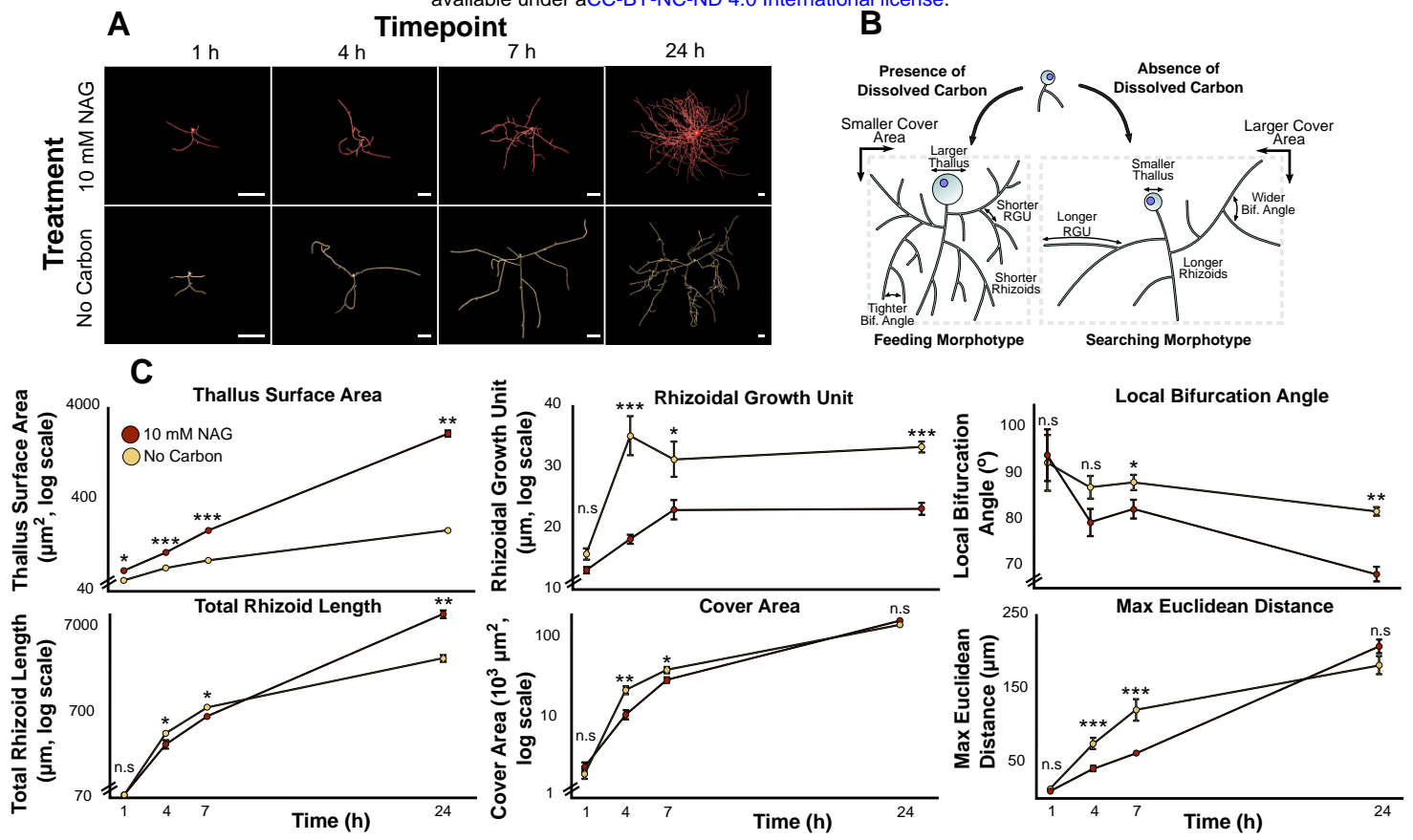
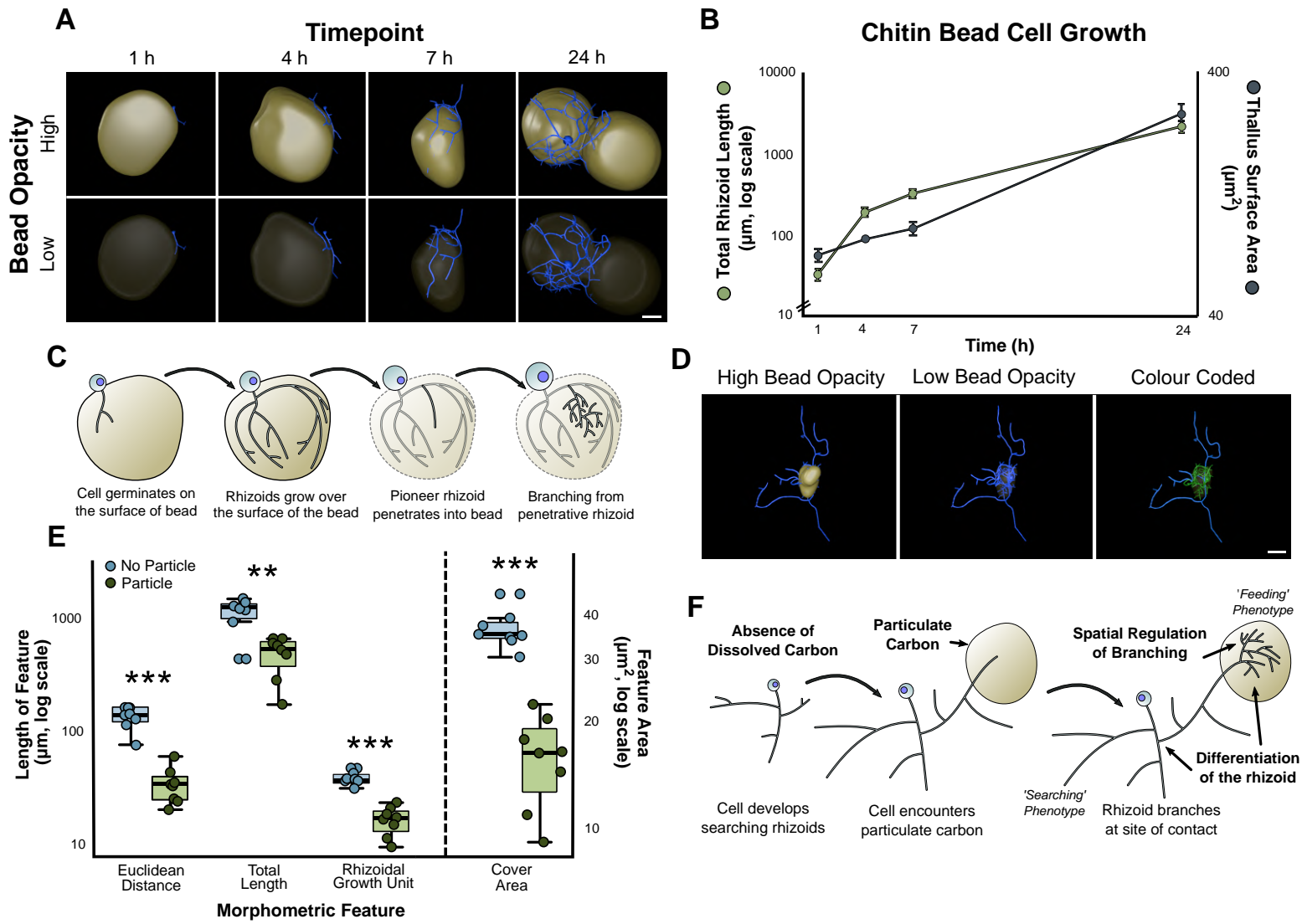


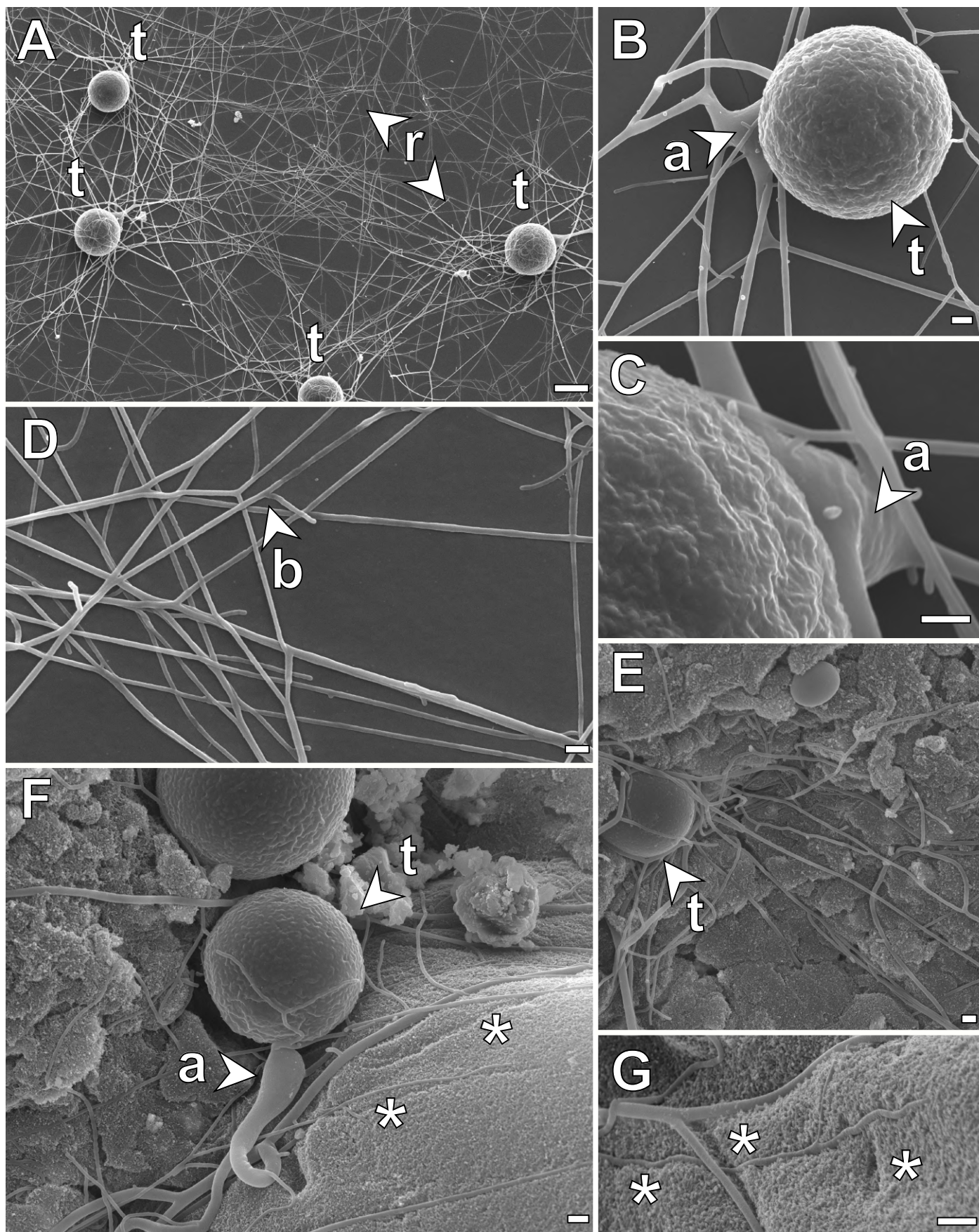
Figure 3



## Figure 4

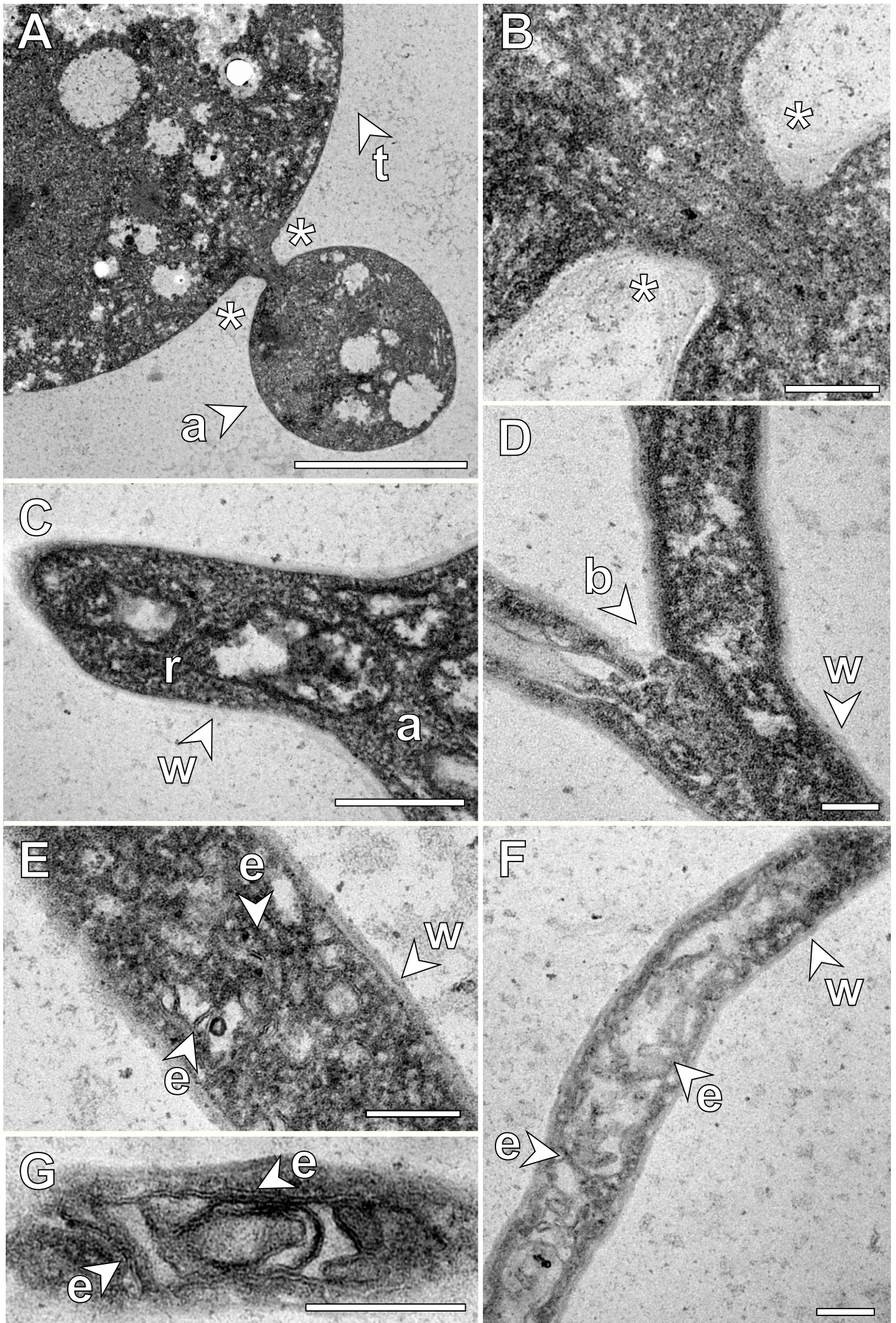


Supplementary Figure 1



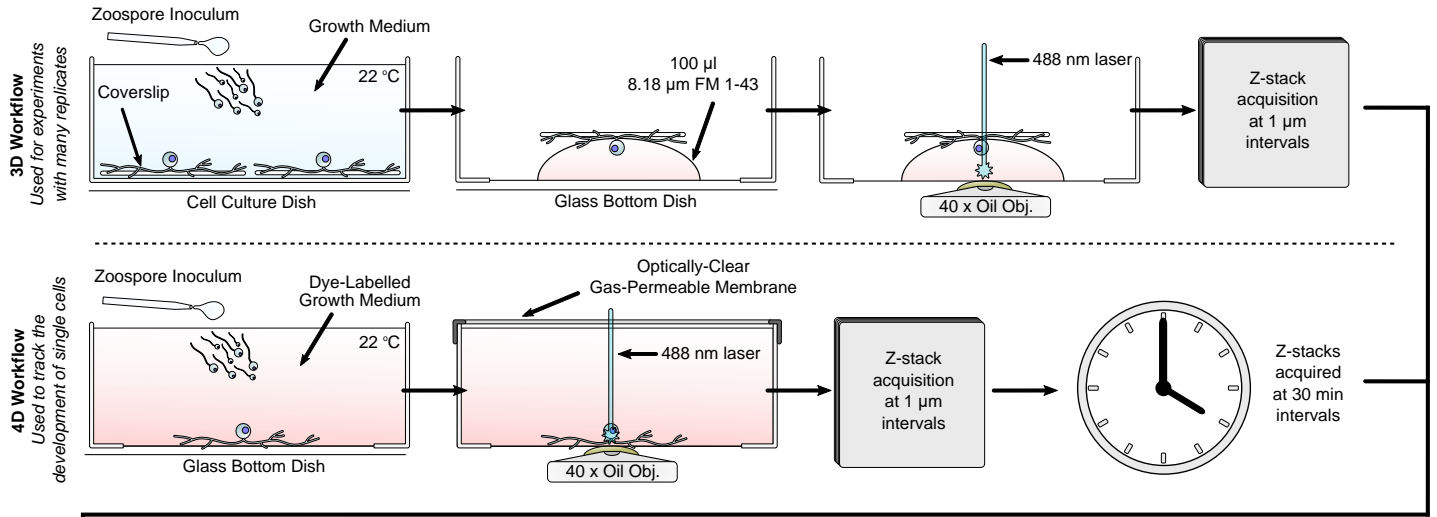


Supplementary Figure 2

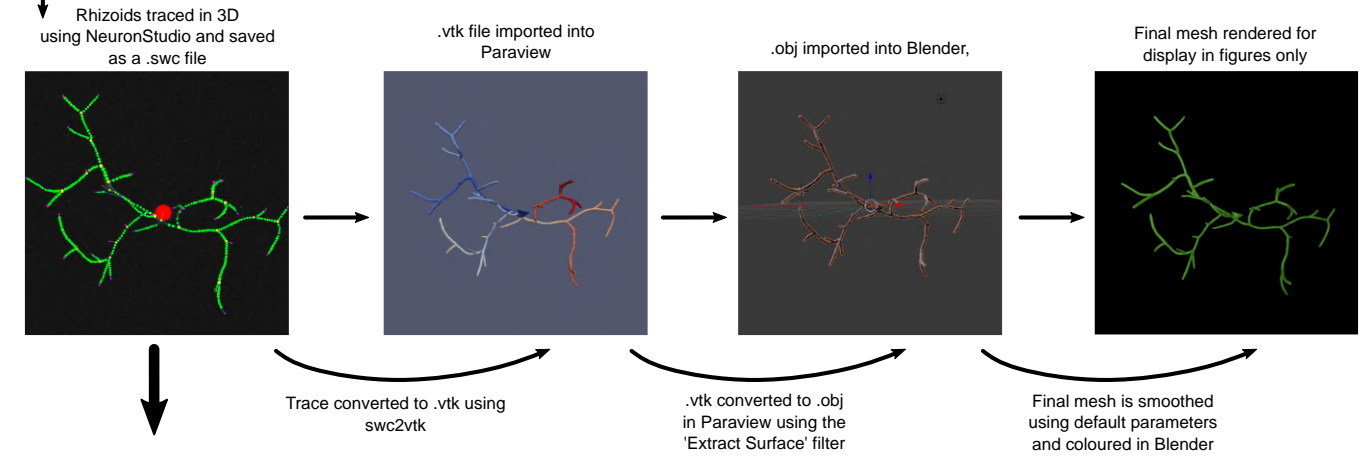


## Supplementary Figure 3

### Acquisition



### Reconstruction

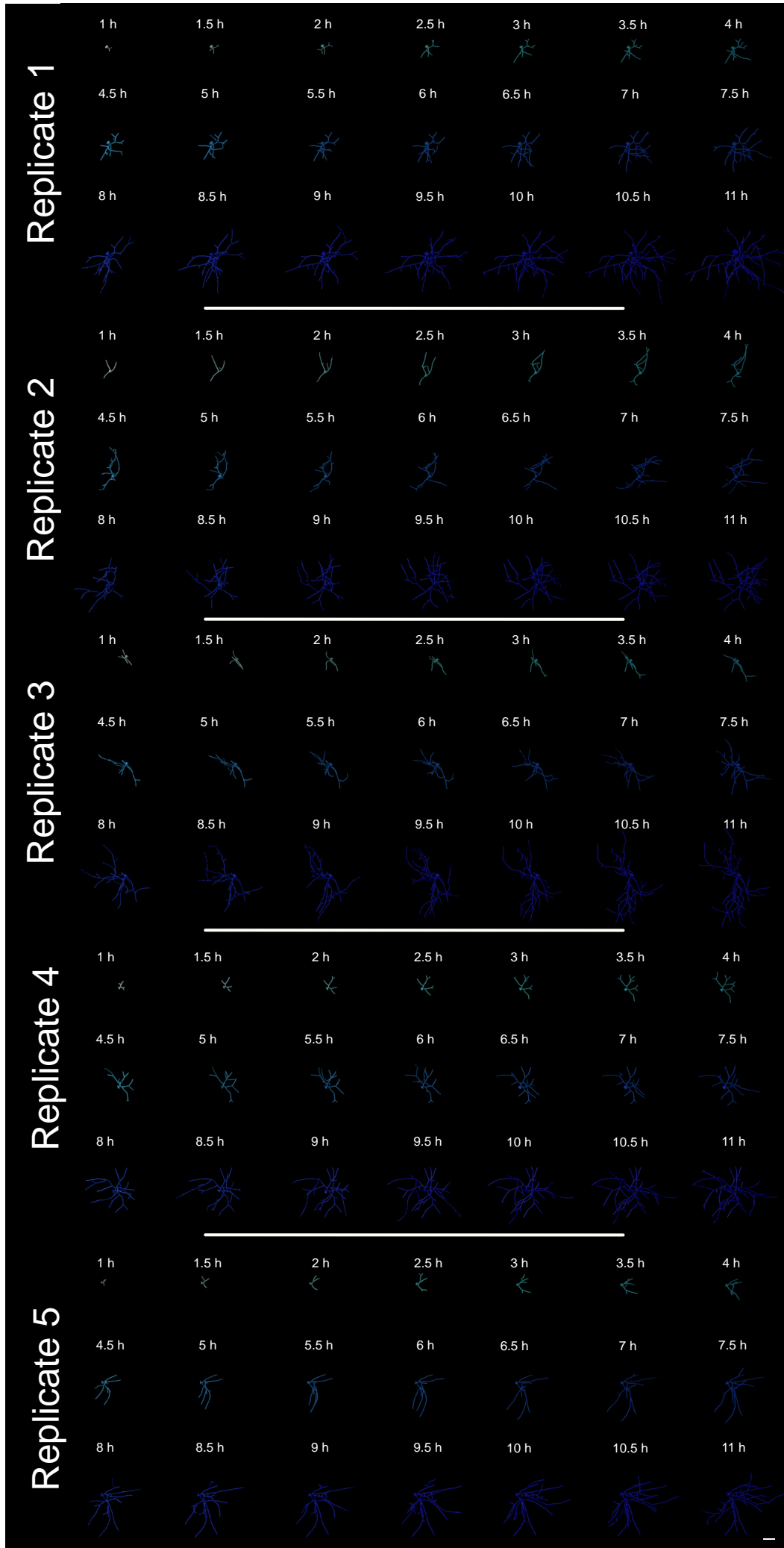


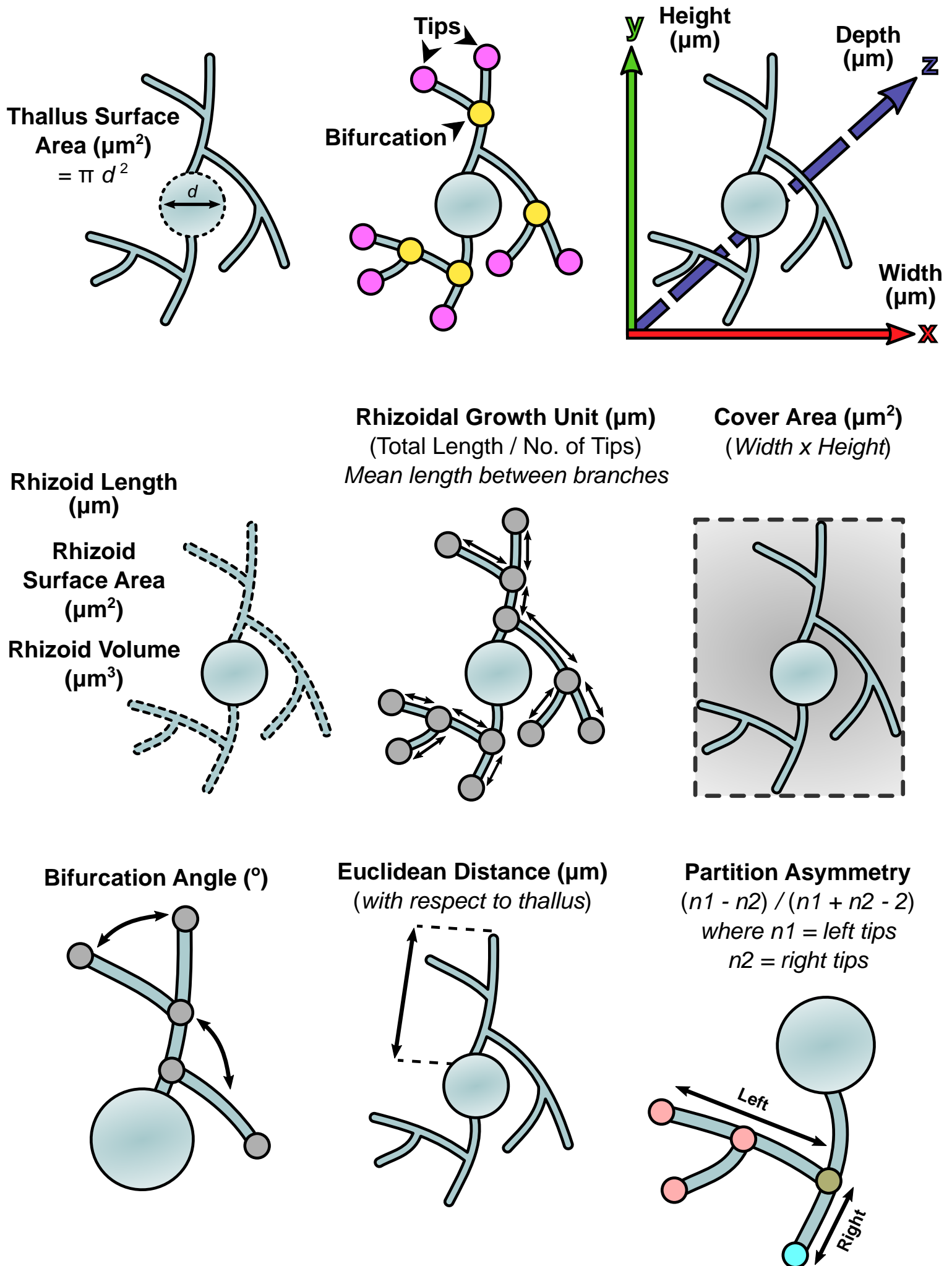
.swc file quantified for morphometric features using `btmorph2` and analysed in R Studio

### Analysis

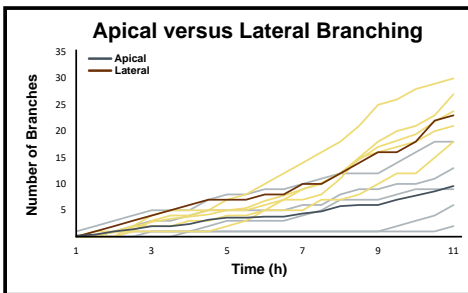
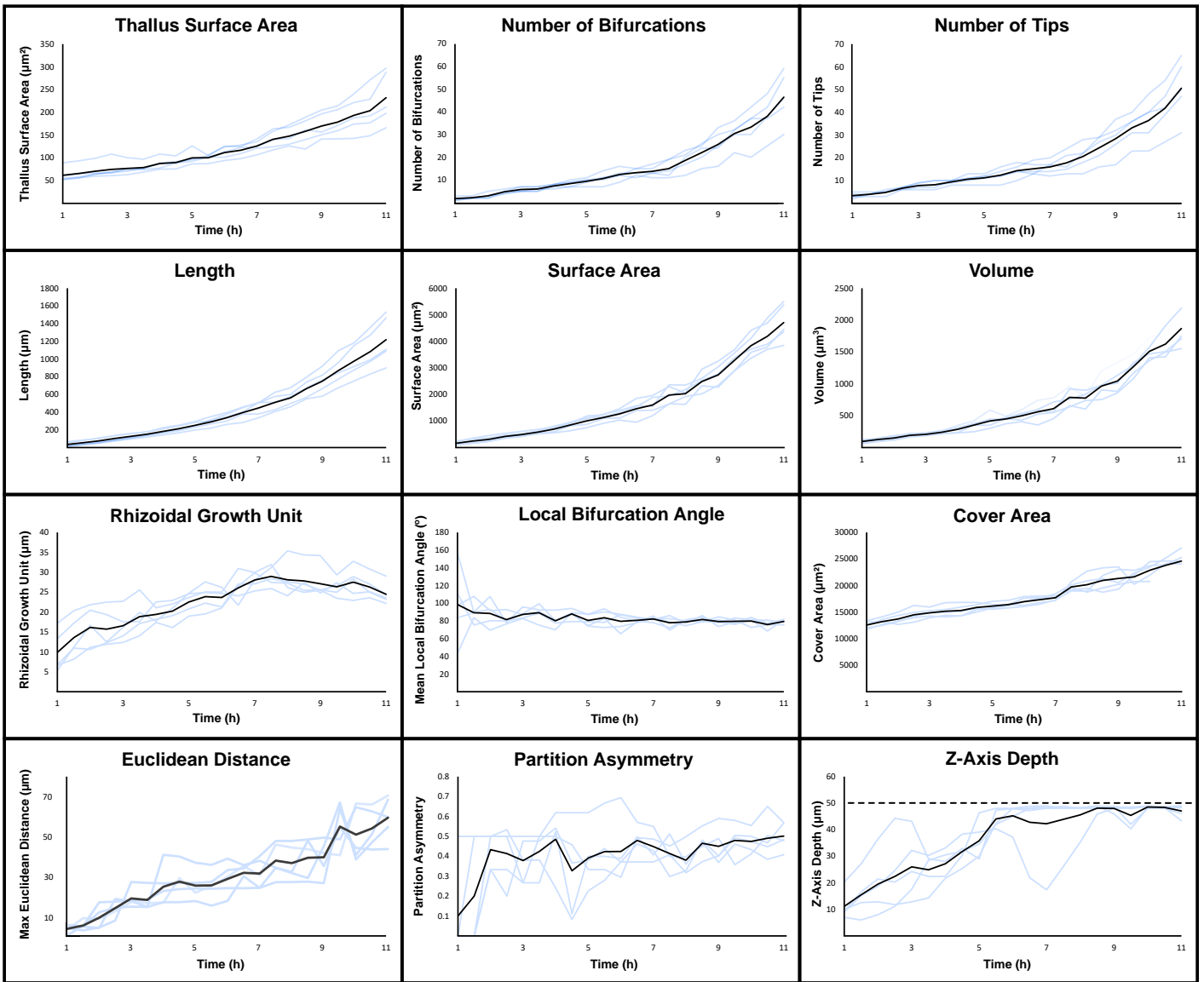
### Visualisation

Supplementary Figure 4





### Supplementary Figure 6

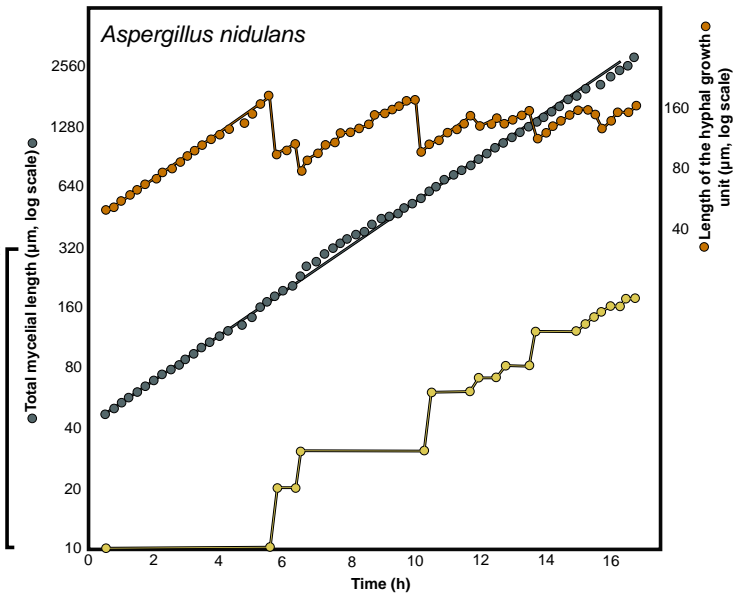
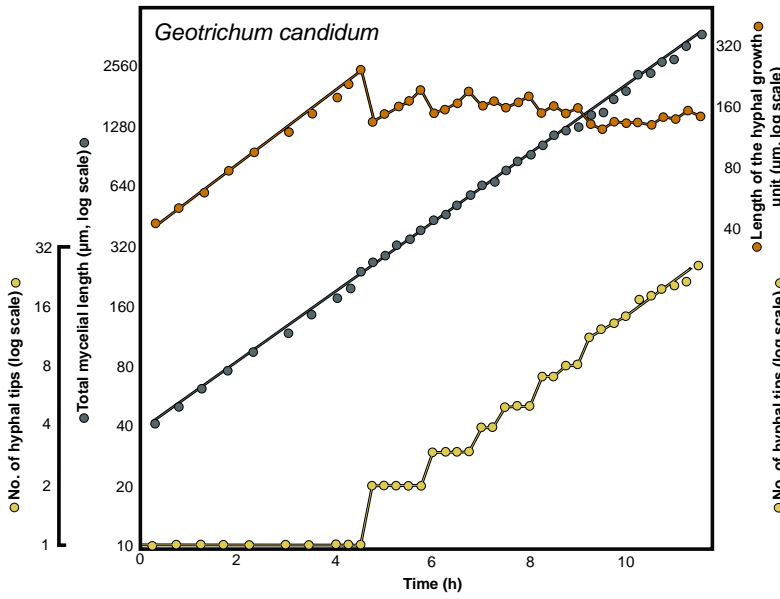


**Ascomycota**

Trinci, 1974

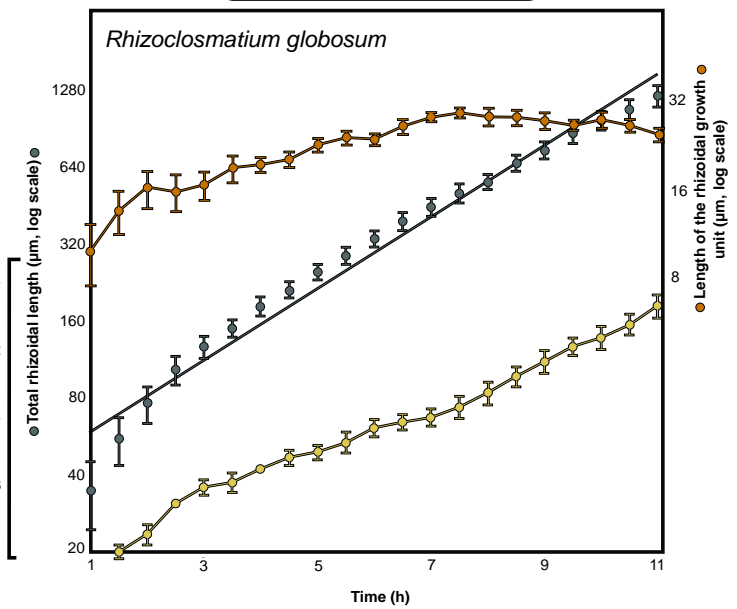
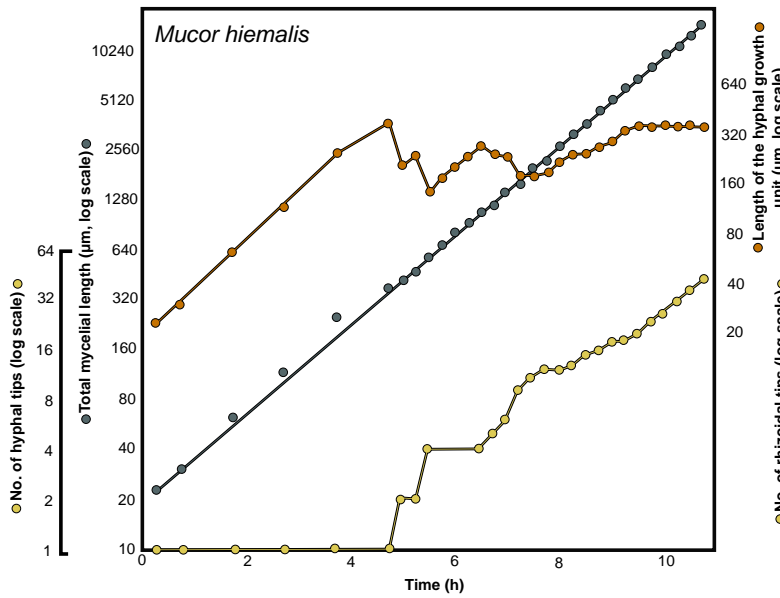
This Study

**Ascomycota**

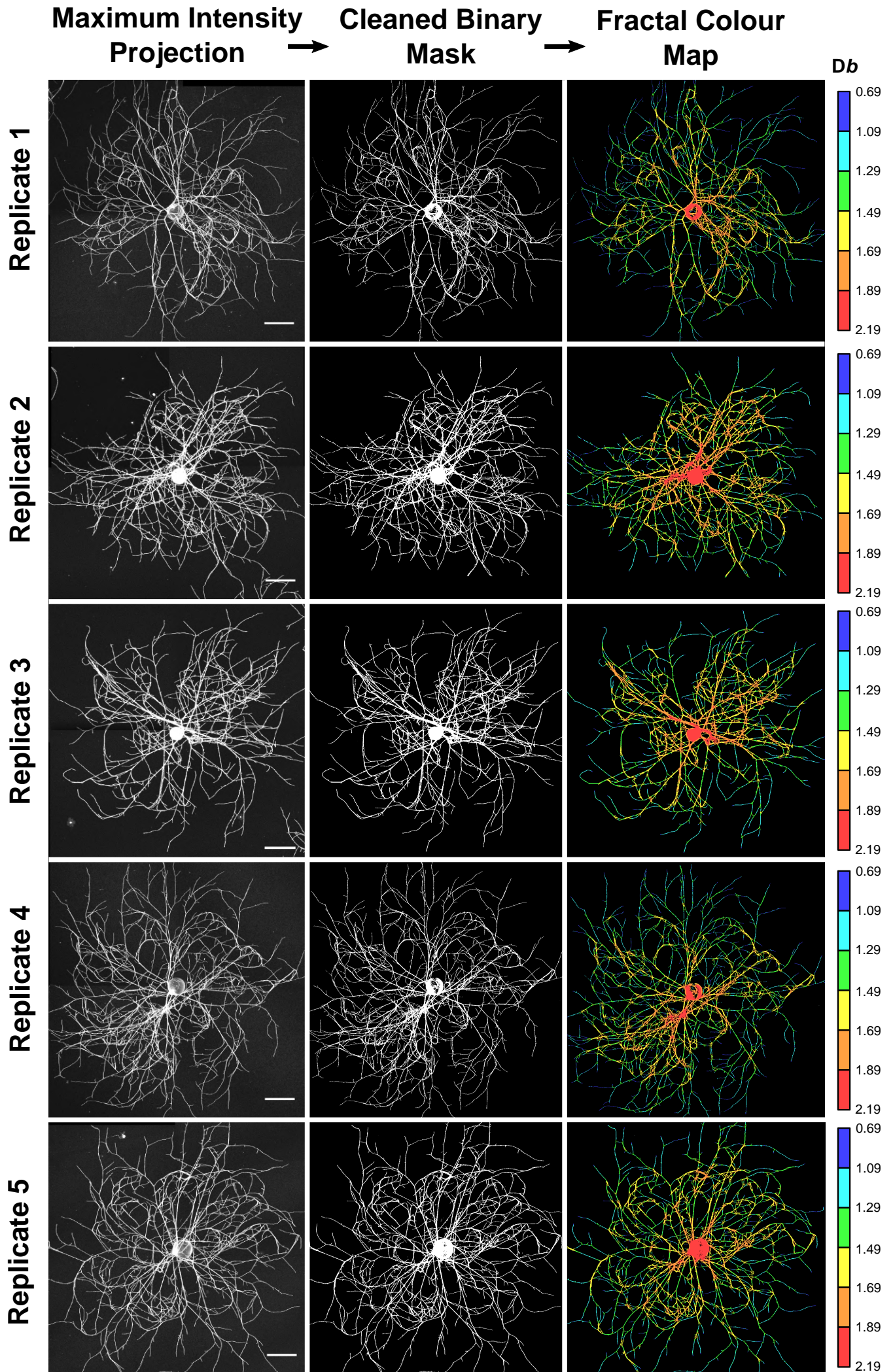


**Mucoromycota**

**Chytridiomycota**



Supplementary Figure 8



Supplementary Table 1

| <b>4D Development</b>                    |                                 |   |                                 |   |                                 |   |
|--|---------------------------------|---|---------------------------------|---|---------------------------------|---|
| <b>Morphometric Feature</b>              | <b>(1 h)</b><br><b>(Mean)</b>   | <b>±</b><br><b>Standard</b><br><b>Deviation</b> | <b>(1.5 h)</b><br><b>(Mean)</b> | <b>±</b><br><b>Standard</b><br><b>Deviation</b> | <b>(2 h)</b><br><b>(Mean)</b>   | <b>±</b><br><b>Standard</b><br><b>Deviation</b> |
| Thallus Diameter ( $\mu\text{m}^2$ )     | 61.73                           | 15.55   | 65.73                           | 15.90   | 70.65                           | 15.91   |
| Number of Bifurcations                   | 1.80                            | 0.84  | 2.20                            | 0.45  | 3.00                            | 1.22  |
| Number of Tips                           | 3.40                            | 1.14  | 4.00                            | 0.71  | 4.80                            | 1.10  |
| Width ( $\mu\text{m}$ )                  | 115.28                          | 2.31  | 118.40                          | 0.76  | 120.92                          | 1.52  |
| Height ( $\mu\text{m}$ )                 | 108.89                          | 4.02  | 111.68                          | 5.43  | 113.31                          | 7.81  |
| Depth ( $\mu\text{m}$ )                  | 11.13                           | 5.23  | 15.48                           | 7.68  | 19.48                           | 10.83   |
| Total Length ( $\mu\text{m}$ )           | 34.96                           | 23.27   | 55.49                           | 26.18   | 76.24                           | 27.57   |
| Surface Area ( $\mu\text{m}^2$ )         | 160.28                          | 67.69   | 242.43                          | 86.65   | 309.83                          | 95.17   |
| Volume ( $\mu\text{m}^3$ )               | 95.35                           | 24.87   | 126.35                          | 24.33   | 150.28                          | 27.20   |
| Rhizoidal Growth Unit ( $\mu\text{m}$ )  | 9.87                            | 5.15  | 13.57                           | 5.02  | 16.16                           | 5.17  |
| Cover Area ( $\mu\text{m}^2$ )           | 12558.93                        | 680.10  | 13222.81                        | 663.30  | 13701.19                        | 945.32  |
| Mean Bifurcation Angle ( $^\circ$ )      | 98.56                           | 41.45   | 89.28                           | 11.85   | 88.46                           | 14.35   |
| Partition Asymmetry                      | 0.10                            | 0.22  | 0.20                            | 0.27  | 0.43                            | 0.09  |
| Max Euclidean Distance ( $\mu\text{m}$ ) | 4.59                            | 2.06  | 6.24                            | 2.21  | 10.10                           | 5.36  |
| Max Path Distance ( $\mu\text{m}$ )      | 4.92                            | 2.43  | 7.21                            | 2.93  | 11.50                           | 5.88  |
| Number of Apical Branches                | 0.20                            | 0.45  | 0.40                            | 0.89  | 1.00                            | 1.22  |
| Number of Lateral Branches               | 0.00                            | 0.00  | 0.40                            | 0.55  | 0.80                            | 0.84  |
|  | <b>(2.5 h)</b><br><b>(Mean)</b> | <b>±</b><br><b>Standard</b><br><b>Deviation</b> | <b>(3 h)</b><br><b>(Mean)</b>   | <b>±</b><br><b>Standard</b><br><b>Deviation</b> | <b>(3.5 h)</b><br><b>(Mean)</b> | <b>±</b><br><b>Standard</b><br><b>Deviation</b> |
| Thallus Diameter ( $\mu\text{m}^2$ )     | 74.64                           | 19.18   | 80.28                           | 13.97   | 78.74                           | 10.72   |



|  |               |                         |                |                         |               |                         |
|--|---------------|-------------------------|----------------|-------------------------|---------------|-------------------------|
| Number of Bifurcations                   | 4.80          | 0.84                    | 6.00           | 1.10                    | 6.00          | 1.00                    |
| Number of Tips                           | 6.60          | 0.55                    | 8.17           | 1.30                    | 8.20          | 1.79                    |
| Width ( $\mu\text{m}$ )                  | 124.56        | 1.06                    | 126.69         | 2.62                    | 127.67        | 2.68                    |
| Height ( $\mu\text{m}$ )                 | 116.33        | 9.44                    | 117.53         | 8.31                    | 118.83        | 10.80                   |
| Depth ( $\mu\text{m}$ )                  | 22.43         | 13.50                   | 24.05          | 12.05                   | 24.90         | 6.66                    |
| Total Length ( $\mu\text{m}$ )           | 103.01        | 29.69                   | 129.64         | 28.92                   | 150.42        | 26.09                   |
| Surface Area ( $\mu\text{m}^2$ )         | 419.67        | 78.87                   | 498.16         | 80.13                   | 579.40        | 69.78                   |
| Volume ( $\mu\text{m}^3$ )               | 191.82        | 25.09                   | 216.88         | 19.13                   | 239.34        | 23.15                   |
| Rhizoidal Growth Unit ( $\mu\text{m}$ )  | 15.72         | 4.89                    | 16.14          | 3.97                    | 18.85         | 4.29                    |
| Cover Area ( $\mu\text{m}^2$ )           | 14489.81      | 1178.25                 | 14876.19       | 798.19                  | 15148.16      | 1056.39                 |
| Mean Bifurcation Angle ( $^\circ$ )      | 81.51         | 6.51                    | 85.40          | 5.20                    | 89.34         | 8.82                    |
| Partition Asymmetry                      | 0.41          | 0.14                    | 0.39           | 0.11                    | 0.42          | 0.10                    |
| Max Euclidean Distance ( $\mu\text{m}$ ) | 14.85         | 4.23                    | 19.28          | 4.71                    | 18.90         | 4.97                    |
| Max Path Distance ( $\mu\text{m}$ )      | 18.14         | 5.13                    | 23.20          | 5.13                    | 23.75         | 5.18                    |
| Number of Apical Branches                | 1.40          | 1.67                    | 2.50           | 2.00                    | 2.00          | 2.00                    |
| Number of Lateral Branches               | 1.80          | 0.84                    | 3.00           | 1.30                    | 3.40          | 1.82                    |
|  | <b>(4 h)</b>  | <b><math>\pm</math></b> | <b>(4.5 h)</b> | <b><math>\pm</math></b> | <b>(5 h)</b>  | <b><math>\pm</math></b> |
|  | <b>(Mean)</b> | <b>Standard</b>         | <b>(Mean)</b>  | <b>Standard</b>         | <b>(Mean)</b> | <b>Standard</b>         |
|  |               | <b>Deviation</b>        |                | <b>Deviation</b>        |               | <b>Deviation</b>        |
| Thallus Diameter ( $\mu\text{m}^2$ )     | 87.55         | 13.18                   | 89.84          | 10.18                   | 99.90         | 15.33                   |
| Number of Bifurcations                   | 7.40          | 0.89                    | 8.40           | 1.34                    | 9.40          | 1.52                    |
| Number of Tips                           | 9.40          | 0.89                    | 10.60          | 1.82                    | 11.20         | 1.92                    |
| Width ( $\mu\text{m}$ )                  | 128.49        | 4.98                    | 130.81         | 6.80                    | 133.09        | 8.08                    |
| Height ( $\mu\text{m}$ )                 | 119.48        | 13.29                   | 121.85         | 11.97                   | 121.57        | 10.10                   |
| Depth ( $\mu\text{m}$ )                  | 27.16         | 5.01                    | 31.81          | 4.67                    | 35.82         | 7.13                    |
| Total Length ( $\mu\text{m}$ )           | 183.21        | 34.22                   | 212.60         | 35.17                   | 250.30        | 39.92                   |

|  |                |                         |               |                         |                |                         |
|--|----------------|-------------------------|---------------|-------------------------|----------------|-------------------------|
| Surface Area ( $\mu\text{m}^2$ )         | 697.97         | 112.24                  | 856.05        | 134.33                  | 1004.34        | 184.45                  |
| Volume ( $\mu\text{m}^3$ )               | 286.28         | 51.44                   | 351.77        | 63.07                   | 416.94         | 108.92                  |
| Rhizoidal Growth Unit ( $\mu\text{m}$ )  | 19.40          | 2.28                    | 20.23         | 2.71                    | 22.54          | 2.55                    |
| Cover Area ( $\mu\text{m}^2$ )           | 15298.59       | 1096.41                 | 15874.79      | 707.32                  | 16119.89       | 603.53                  |
| Mean Bifurcation Angle ( $^\circ$ )      | 80.11          | 7.99                    | 87.90         | 5.39                    | 80.59          | 6.54                    |
| Partition Asymmetry                      | 0.49           | 0.14                    | 0.33          | 0.23                    | 0.39           | 0.14                    |
| Max Euclidean Distance ( $\mu\text{m}$ ) | 25.42          | 9.73                    | 27.94         | 8.30                    | 26.01          | 7.13                    |
| Max Path Distance ( $\mu\text{m}$ )      | 30.92          | 11.74                   | 35.03         | 10.52                   | 34.40          | 11.86                   |
| Number of Apical Branches                | 2.40           | 1.95                    | 3.20          | 2.68                    | 3.60           | 2.97                    |
| Number of Lateral Branches               | 3.80           | 1.92                    | 4.20          | 2.28                    | 5.00           | 2.12                    |
|  | <b>(5.5 h)</b> | <b><math>\pm</math></b> | <b>(6 h)</b>  | <b><math>\pm</math></b> | <b>(6.5 h)</b> | <b><math>\pm</math></b> |
|  | <b>(Mean)</b>  | <b>Standard</b>         | <b>(Mean)</b> | <b>Standard</b>         | <b>(Mean)</b>  | <b>Standard</b>         |
|  |                | <b>Deviation</b>        |               | <b>Deviation</b>        |                | <b>Deviation</b>        |
| Thallus Diameter ( $\mu\text{m}^2$ )     | 100.34         | 7.52                    | 111.63        | 13.83                   | 116.66         | 12.51                   |
| Number of Bifurcations                   | 10.60          | 2.51                    | 12.40         | 2.51                    | 13.20          | 1.79                    |
| Number of Tips                           | 12.40          | 2.97                    | 14.40         | 2.97                    | 15.20          | 2.68                    |
| Width ( $\mu\text{m}$ )                  | 134.75         | 8.19                    | 137.86        | 8.19                    | 141.14         | 9.67                    |
| Height ( $\mu\text{m}$ )                 | 122.19         | 8.54                    | 123.33        | 8.78                    | 123.15         | 8.15                    |
| Depth ( $\mu\text{m}$ )                  | 44.05          | 3.44                    | 45.24         | 4.66                    | 42.83          | 11.70                   |
| Total Length ( $\mu\text{m}$ )           | 290.01         | 48.65                   | 336.86        | 55.51                   | 394.34         | 70.39                   |
| Surface Area ( $\mu\text{m}^2$ )         | 1131.95        | 138.18                  | 1268.24       | 186.91                  | 1460.13        | 325.84                  |
| Volume ( $\mu\text{m}^3$ )               | 448.43         | 45.57                   | 497.52        | 79.06                   | 560.30         | 140.57                  |
| Rhizoidal Growth Unit ( $\mu\text{m}$ )  | 23.87          | 3.07                    | 23.65         | 2.33                    | 26.07          | 3.45                    |
| Cover Area ( $\mu\text{m}^2$ )           | 16414.85       | 525.82                  | 16960.99      | 817.17                  | 17329.43       | 639.39                  |
| Mean Bifurcation Angle ( $^\circ$ )      | 83.58          | 8.62                    | 79.63         | 9.66                    | 80.75          | 2.71                    |
| Partition Asymmetry                      | 0.42           | 0.15                    | 0.42          | 0.16                    | 0.48           | 0.07                    |

|  |               |                         |                |                         |               |                         |
|--|---------------|-------------------------|----------------|-------------------------|---------------|-------------------------|
| Max Euclidean Distance ( $\mu\text{m}$ ) | 26.12         | 7.24                    | 29.34          | 8.08                    | 32.36         | 4.80                    |
| Max Path Distance ( $\mu\text{m}$ )      | 35.29         | 10.43                   | 39.00          | 12.77                   | 44.57         | 8.77                    |
| Number of Apical Branches                | 3.60          | 2.97                    | 3.80           | 3.35                    | 3.80          | 3.35                    |
| Number of Lateral Branches               | 5.40          | 2.07                    | 6.80           | 2.17                    | 7.80          | 2.59                    |
|  | <b>(7 h)</b>  | <b><math>\pm</math></b> | <b>(7.5 h)</b> | <b><math>\pm</math></b> | <b>(8 h)</b>  | <b><math>\pm</math></b> |
|  | <b>(Mean)</b> | <b>Standard</b>         | <b>(Mean)</b>  | <b>Standard</b>         | <b>(Mean)</b> | <b>Standard</b>         |
|  |               | <b>Deviation</b>        |                | <b>Deviation</b>        |               | <b>Deviation</b>        |
| Thallus Diameter ( $\mu\text{m}^2$ )     | 125.80        | 13.55                   | 140.79         | 20.30                   | 153.26        | 21.19                   |
| Number of Bifurcations                   | 13.80         | 2.28                    | 15.00          | 3.81                    | 19.83         | 4.28                    |
| Number of Tips                           | 16.00         | 3.08                    | 17.80          | 4.55                    | 22.00         | 5.55                    |
| Width ( $\mu\text{m}$ )                  | 144.14        | 10.96                   | 149.97         | 9.68                    | 150.13        | 11.91                   |
| Height ( $\mu\text{m}$ )                 | 123.26        | 6.90                    | 131.91         | 7.67                    | 136.32        | 9.30                    |
| Depth ( $\mu\text{m}$ )                  | 42.26         | 13.92                   | 43.90          | 9.92                    | 46.12         | 5.77                    |
| Total Length ( $\mu\text{m}$ )           | 447.68        | 83.46                   | 507.96         | 93.67                   | 590.88        | 85.01                   |
| Surface Area ( $\mu\text{m}^2$ )         | 1602.52       | 321.61                  | 1977.68        | 343.82                  | 2181.31       | 275.48                  |
| Volume ( $\mu\text{m}^3$ )               | 609.97        | 132.73                  | 786.87         | 146.15                  | 847.84        | 112.19                  |
| Rhizoidal Growth Unit ( $\mu\text{m}$ )  | 28.05         | 1.97                    | 28.96          | 2.52                    | 27.66         | 4.29                    |
| Cover Area ( $\mu\text{m}^2$ )           | 17710.48      | 522.73                  | 19733.66       | 687.82                  | 20439.86      | 1649.74                 |
| Mean Bifurcation Angle ( $^\circ$ )      | 82.27         | 2.76                    | 77.85          | 6.87                    | 78.96         | 2.85                    |
| Partition Asymmetry                      | 0.45          | 0.07                    | 0.41           | 0.08                    | 0.40          | 0.07                    |
| Max Euclidean Distance ( $\mu\text{m}$ ) | 31.95         | 7.37                    | 38.37          | 8.62                    | 38.31         | 8.82                    |
| Max Path Distance ( $\mu\text{m}$ )      | 44.88         | 11.89                   | 53.08          | 14.99                   | 55.74         | 13.07                   |
| Number of Apical Branches                | 4.40          | 3.78                    | 4.80           | 4.15                    | 6.83          | 4.76                    |
| Number of Lateral Branches               | 9.00          | 3.39                    | 10.20          | 3.49                    | 12.50         | 3.94                    |

|  | <b>(8.5 h)</b><br><b>(Mean)</b> | <b>±</b><br><b>Standard</b><br><b>Deviation</b> | <b>(9 h)</b><br><b>(Mean)</b>    | <b>±</b><br><b>Standard</b><br><b>Deviation</b> | <b>(9.5 h)</b><br><b>(Mean)</b> | <b>±</b><br><b>Standard</b><br><b>Deviation</b> |
|--|---------------------------------|---|----------------------------------|---|---------------------------------|---|
| Thallus Diameter ( $\mu\text{m}^2$ )     | 158.24                          | 28.84   | 169.98                           | 28.77   | 178.45                          | 30.65   |
| Number of Bifurcations                   | 22.00                           | 4.53  | 25.60                            | 6.50  | 30.40                           | 5.18  |
| Number of Tips                           | 24.40                           | 5.73  | 28.40                            | 7.50  | 33.20                           | 6.53  |
| Width ( $\mu\text{m}$ )                  | 153.49                          | 15.50   | 154.51                           | 15.11   | 157.71                          | 17.56   |
| Height ( $\mu\text{m}$ )                 | 136.95                          | 9.97  | 138.78                           | 14.09   | 137.92                          | 9.11  |
| Depth ( $\mu\text{m}$ )                  | 48.11                           | 1.32  | 48.03                            | 1.18  | 45.40                           | 3.89  |
| Total Length ( $\mu\text{m}$ )           | 664.75                          | 106.31  | 749.34                           | 131.57  | 869.09                          | 162.80  |
| Surface Area ( $\mu\text{m}^2$ )         | 2484.50                         | 341.81  | 2736.00                          | 427.52  | 3290.47                         | 372.99  |
| Volume ( $\mu\text{m}^3$ )               | 963.75                          | 163.46  | 1043.59                          | 195.90  | 1269.05                         | 150.26  |
| Rhizoidal Growth Unit ( $\mu\text{m}$ )  | 27.84                           | 3.78  | 27.12                            | 3.95  | 26.35                           | 2.25  |
| Cover Area ( $\mu\text{m}^2$ )           | 20955.39                        | 1838.27   | 21331.96                         | 1840.64   | 21626.97                        | 1102.86   |
| Mean Bifurcation Angle ( $^\circ$ )      | 81.69                           | 3.23  | 79.24                            | 4.05  | 79.52                           | 2.78  |
| Partition Asymmetry                      | 0.47                            | 0.06  | 0.45                             | 0.09  | 0.48                            | 0.08  |
| Max Euclidean Distance ( $\mu\text{m}$ ) | 39.80                           | 10.19   | 40.08                            | 8.86  | 55.31                           | 10.81   |
| Max Path Distance ( $\mu\text{m}$ )      | 55.92                           | 12.69   | 57.55                            | 16.95   | 74.23                           | 12.13   |
| Number of Apical Branches                | 6.00                            | 4.90  | 6.00                             | 4.90  | 7.00                            | 5.48  |
| Number of Lateral Branches               | 14.60                           | 4.62  | 17.00                            | 5.39  | 18.20                           | 5.22  |
|  | <b>(10 h)</b><br><b>(Mean)</b>  | <b>±</b><br><b>Standard</b><br><b>Deviation</b> | <b>(10.5 h)</b><br><b>(Mean)</b> | <b>±</b><br><b>Standard</b><br><b>Deviation</b> | <b>(11 h)</b><br><b>(Mean)</b>  | <b>±</b><br><b>Standard</b><br><b>Deviation</b> |
| Thallus Diameter ( $\mu\text{m}^2$ )     | 193.39                          | 38.51   | 203.54                           | 47.69   | 232.18                          | 57.64   |
| Number of Bifurcations                   | 33.20                           | 8.53  | 38.00                            | 8.46  | 46.40                           | 11.41   |
| Number of Tips                           | 36.40                           | 9.61  | 41.80                            | 10.03   | 50.60                           | 13.16   |

|  |          |         |          |         |          |         |
|--|----------|---------|----------|---------|----------|---------|
| Width ( $\mu\text{m}$ )                  | 166.25   | 21.27   | 168.86   | 22.61   | 170.74   | 25.31   |
| Height ( $\mu\text{m}$ )                 | 138.76   | 12.08   | 142.45   | 15.78   | 145.67   | 16.12   |
| Depth ( $\mu\text{m}$ )                  | 48.55    | 0.42    | 48.39    | 0.30    | 47.04    | 2.34    |
| Total Length ( $\mu\text{m}$ )           | 977.64   | 186.20  | 1084.53  | 220.20  | 1219.15  | 268.22  |
| Surface Area ( $\mu\text{m}^2$ )         | 3836.65  | 422.94  | 4187.25  | 549.42  | 4707.64  | 704.53  |
| Volume ( $\mu\text{m}^3$ )               | 1510.22  | 145.44  | 1623.77  | 209.37  | 1868.34  | 280.25  |
| Rhizoidal Growth Unit ( $\mu\text{m}$ )  | 27.51    | 3.84    | 26.30    | 2.78    | 24.48    | 2.67    |
| Cover Area ( $\mu\text{m}^2$ )           | 22884.73 | 1500.84 | 23811.10 | 1536.94 | 24595.64 | 1879.28 |
| Mean Bifurcation Angle ( $^\circ$ )      | 79.91    | 4.24    | 75.90    | 4.53    | 79.41    | 2.45    |
| Partition Asymmetry                      | 0.47     | 0.06    | 0.49     | 0.10    | 0.50     | 0.07    |
| Max Euclidean Distance ( $\mu\text{m}$ ) | 51.27    | 13.40   | 54.37    | 9.71    | 59.69    | 10.78   |
| Max Path Distance ( $\mu\text{m}$ )      | 72.72    | 13.07   | 78.64    | 11.26   | 86.12    | 12.58   |
| Number of Apical Branches                | 7.80     | 5.97    | 8.60     | 6.58    | 9.60     | 6.19    |
| Number of Lateral Branches               | 19.40    | 5.81    | 21.80    | 5.07    | 23.80    | 4.76    |

Supplementary Table 2

| <b>1 <math>\mu\text{M}</math> Caspofungin Diacetate Morphometric Feature</b>  | <b>Poisoned Cells (Mean)</b> | <b><math>\pm</math> Standard Deviation</b> | <b>Control Cells (Mean)</b> | <b><math>\pm</math> Standard Deviation</b> | <b>t-test p-value</b> |
|---|------------------------------|--|-----------------------------|--|-----------------------|
| Thallus Diameter ( $\mu\text{m}^2$ )  | 156.35                       | 33.59                                      | 149.01                      | 12.84                                      | $p > 0.05$            |
| Number of Bifurcations  | 22.25                        | 5.26                                       | 20.75                       | 3.73                                       | $p > 0.05$            |
| Number of Tips  | 25.63                        | 6.16                                       | 23.38                       | 3.29                                       | $p > 0.05$            |
| Width ( $\mu\text{m}$ )   | 171.95                       | 23.36                                      | 183.52                      | 20.38                                      | $p > 0.05$            |
| Height ( $\mu\text{m}$ )  | 149.81                       | 16.35                                      | 166.01                      | 12.42                                      | $p < 0.05$            |
| Depth ( $\mu\text{m}$ )   | 14.84                        | 5.98                                       | 12.85                       | 2.09                                       | $p > 0.05$            |
| Total Length ( $\mu\text{m}$ )  | 558.41                       | 113.78                                     | 511.62                      | 117.53                                     | $p > 0.05$            |
| Surface Area ( $\mu\text{m}^2$ )  | 2188.88                      | 922.56                                     | 2019.66                     | 312.08                                     | $p > 0.05$            |
| Volume ( $\mu\text{m}^3$ )  | 927.54                       | 561.11                                     | 841.85                      | 139.38                                     | $p > 0.05$            |
| Rhizoidal Growth Unit ( $\mu\text{m}$ )                                       | 22.08                        | 2.13                                       | 21.88                       | 3.83                                       | $p > 0.05$            |
| Cover Area ( $\mu\text{m}^2$ )  | 25841.89                     | 4907.30                                    | 30447.12                    | 4005.04                                    | $p > 0.05$            |
| Mean Bifurcation Angle ( $^\circ$ )   | 83.87                        | 7.23                                       | 77.41                       | 4.13                                       | $p > 0.05$            |
| Partition Asymmetry   | 0.65                         | 0.06                                       | 0.61                        | 0.08                                       | $p > 0.05$            |
| Max Euclidean Distance ( $\mu\text{m}$ )                                      | 58.60                        | 12.95                                      | 60.06                       | 13.31                                      | $p > 0.05$            |
| Max Path Distance ( $\mu\text{m}$ )   | 89.46                        | 27.71                                      | 69.70                       | 15.94                                      | $p > 0.05$            |
| <b>10 <math>\mu\text{M}</math> Caspofungin Diacetate Morphometric Feature</b> | <b>Poisoned Cells (Mean)</b> | <b><math>\pm</math> Standard Deviation</b> | <b>Control Cells (Mean)</b> | <b><math>\pm</math> Standard Deviation</b> | <b>t-test p-value</b> |
| Thallus Diameter ( $\mu\text{m}^2$ )  | 116.66                       | 10.21                                      | 146.81                      | 8.06                                       | $p < 0.001$           |
| Number of Bifurcations  | 16.38                        | 4.21                                       | 22.75                       | 4.50                                       | $p < 0.05$            |
| Number of Tips  | 20.00                        | 4.72                                       | 25.50                       | 3.93                                       | $p < 0.05$            |
| Width ( $\mu\text{m}$ )   | 147.69                       | 18.06                                      | 178.64                      | 28.42                                      | $p < 0.05$            |
| Height ( $\mu\text{m}$ )  | 117.83                       | 21.04                                      | 158.94                      | 27.44                                      | $p < 0.01$            |
| Depth ( $\mu\text{m}$ )   | 9.73                         | 2.93                                       | 12.66                       | 2.56                                       | $p > 0.05$            |
| Total Length ( $\mu\text{m}$ )  | 236.11                       | 56.46                                      | 507.82                      | 60.22                                      | $p < 0.001$           |
| Surface Area ( $\mu\text{m}^2$ )  | 778.83                       | 168.46                                     | 1938.29                     | 176.30                                     | $p < 0.001$           |
| Volume ( $\mu\text{m}^3$ )  | 335.65                       | 62.71                                      | 780.04                      | 56.72                                      | $p < 0.001$           |
| Rhizoidal Growth Unit ( $\mu\text{m}$ )                                       | 11.91                        | 2.20                                       | 20.41                       | 4.22                                       | $p < 0.001$           |
| Cover Area ( $\mu\text{m}^2$ )  | 17415.38                     | 4017.82                                    | 28280.04                    | 6059.43                                    | $p < 0.01$            |
| Mean Bifurcation Angle ( $^\circ$ )   | 82.95                        | 7.60                                       | 83.81                       | 5.53                                       | $p > 0.05$            |
| Partition Asymmetry   | 0.43                         | 0.20                                       | 0.69                        | 0.07                                       | $p < 0.01$            |
| Max Euclidean Distance ( $\mu\text{m}$ )                                      | 27.08                        | 5.83                                       | 59.78                       | 8.10                                       | $p < 0.001$           |
| Max Path Distance ( $\mu\text{m}$ )   | 35.56                        | 7.84                                       | 67.72                       | 7.82                                       | $p < 0.001$           |

| <b>50 <math>\mu\text{M}</math> Caspofungin Diacetate Morphometric Feature</b> | <b>Poisoned Cells (Mean)</b> | <b><math>\pm</math> Standard Deviation</b> | <b>Control Cells (Mean)</b> | <b><math>\pm</math> Standard Deviation</b> | <b><i>t</i>-test <i>p</i>-value</b> |
|---|------------------------------|--|-----------------------------|--|-------------------------------------|
| Thallus Diameter ( $\mu\text{m}^2$ )  | 102.66                       | 4.58                                       | 138.43                      | 21.87                                      | $p < 0.01$                          |
| Number of Bifurcations  | 12.63                        | 3.38                                       | 20.50                       | 8.28                                       | $p < 0.05$                          |
| Number of Tips  | 15.13                        | 3.36                                       | 23.38                       | 8.21                                       | $p < 0.05$                          |
| Width ( $\mu\text{m}$ )   | 144.14                       | 5.03                                       | 207.57                      | 82.07                                      | $p < 0.05$                          |
| Height ( $\mu\text{m}$ )  | 116.13                       | 24.38                                      | 166.90                      | 81.07                                      | $p < 0.001$                         |
| Depth ( $\mu\text{m}$ )   | 7.41                         | 3.17                                       | 11.87                       | 2.89                                       | $p < 0.05$                          |
| Total Length ( $\mu\text{m}$ )  | 68.02                        | 16.73                                      | 409.88                      | 102.22                                     | $p < 0.001$                         |
| Surface Area ( $\mu\text{m}^2$ )  | 268.76                       | 58.11                                      | 1523.21                     | 576.05                                     | $p < 0.001$                         |
| Volume ( $\mu\text{m}^3$ )  | 182.96                       | 20.38                                      | 664.00                      | 386.28                                     | $p < 0.001$                         |
| Rhizoidal Growth Unit ( $\mu\text{m}$ )                                       | 4.52                         | 0.64                                       | 20.67                       | 13.09                                      | $p < 0.001$                         |
| Cover Area ( $\mu\text{m}^2$ )  | 16742.96                     | 3613.72                                    | 40161.41                    | 43389.89                                   | $p < 0.01$                          |
| Mean Bifurcation Angle ( $^\circ$ )   | 87.60                        | 9.17                                       | 86.20                       | 11.15                                      | $p > 0.05$                          |
| Partition Asymmetry   | 0.53                         | 0.16                                       | 0.60                        | 0.12                                       | $p > 0.05$                          |
| Max Euclidean Distance ( $\mu\text{m}$ )                                      | 14.68                        | 3.36                                       | 43.64                       | 13.05                                      | $p < 0.001$                         |
| Max Path Distance ( $\mu\text{m}$ )   | 18.54                        | 4.36                                       | 57.03                       | 10.59                                      | $p < 0.001$                         |
| <b>0.1 <math>\mu\text{M}</math> Cytochalasin B Morphometric Feature</b>       | <b>Poisoned Cells (Mean)</b> | <b><math>\pm</math> Standard Deviation</b> | <b>Control Cells (Mean)</b> | <b><math>\pm</math> Standard Deviation</b> | <b><i>t</i>-test <i>p</i>-value</b> |
| Thallus Diameter ( $\mu\text{m}^2$ )  | 145.42                       | 16.91                                      | 152.08                      | 16.20                                      | $p > 0.05$                          |
| Number of Bifurcations  | 21.00                        | 3.64                                       | 23.13                       | 4.09                                       | $p > 0.05$                          |
| Number of Tips  | 24.11                        | 3.95                                       | 26.63                       | 4.00                                       | $p > 0.05$                          |
| Width ( $\mu\text{m}$ )   | 163.22                       | 22.88                                      | 165.33                      | 12.90                                      | $p > 0.05$                          |
| Height ( $\mu\text{m}$ )  | 166.00                       | 21.01                                      | 157.67                      | 41.68                                      | $p > 0.05$                          |
| Depth ( $\mu\text{m}$ )   | 7.68                         | 1.63                                       | 11.22                       | 2.83                                       | $p < 0.01$                          |
| Total Length ( $\mu\text{m}$ )  | 423.42                       | 83.00                                      | 449.15                      | 72.78                                      | $p > 0.05$                          |
| Surface Area ( $\mu\text{m}^2$ )  | 1631.14                      | 359.82                                     | 1653.61                     | 228.71                                     | $p > 0.05$                          |
| Volume ( $\mu\text{m}^3$ )  | 684.48                       | 158.14                                     | 693.87                      | 128.98                                     | $p > 0.05$                          |
| Rhizoidal Growth Unit ( $\mu\text{m}$ )                                       | 17.87                        | 3.85                                       | 17.24                       | 4.13                                       | $p > 0.05$                          |
| Cover Area ( $\mu\text{m}^2$ )  | 27253.95                     | 5988.26                                    | 26356.21                    | 8234.10                                    | $p > 0.05$                          |
| Mean Bifurcation Angle ( $^\circ$ )   | 85.37                        | 8.44                                       | 82.42                       | 5.49                                       | $p > 0.05$                          |
| Partition Asymmetry   | 0.65                         | 0.13                                       | 0.68                        | 0.09                                       | $p > 0.05$                          |
| Max Euclidean Distance ( $\mu\text{m}$ )                                      | 47.01                        | 11.52                                      | 55.56                       | 13.49                                      | $p > 0.05$                          |
| Max Path Distance ( $\mu\text{m}$ )   | 59.53                        | 11.47                                      | 67.04                       | 16.50                                      | $p > 0.05$                          |
| <b>1 <math>\mu\text{M}</math> Cytochalasin B Morphometric Feature</b>         | <b>Poisoned Cells (Mean)</b> | <b><math>\pm</math> Standard Deviation</b> | <b>Control Cells (Mean)</b> | <b><math>\pm</math> Standard Deviation</b> | <b><i>t</i>-test <i>p</i>-value</b> |
| Thallus Diameter ( $\mu\text{m}^2$ )  | 151.79                       | 47.97                                      | 146.94                      | 25.68                                      | $p > 0.05$                          |

|   |                 |                         |                |                         |                  |
|---|-----------------|-------------------------|----------------|-------------------------|------------------|
| Number of Bifurcations                            | 22.63           | 11.75                   | 22.13          | 4.70                    | $p > 0.05$       |
| Number of Tips                                    | 27.38           | 12.58                   | 25.38          | 5.07                    | $p > 0.05$       |
| Width ( $\mu\text{m}$ )                           | 155.00          | 28.00                   | 189.01         | 16.61                   | $p < 0.01$       |
| Height ( $\mu\text{m}$ )                          | 125.73          | 33.95                   | 144.44         | 21.41                   | $p > 0.05$       |
| Depth ( $\mu\text{m}$ )                           | 18.21           | 5.57                    | 13.09          | 4.95                    | $p > 0.05$       |
| Total Length ( $\mu\text{m}$ )                    | 355.41          | 222.00                  | 459.83         | 72.31                   | $p > 0.05$       |
| Surface Area ( $\mu\text{m}^2$ )                  | 1422.36         | 1066.42                 | 1994.94        | 353.44                  | $p > 0.05$       |
| Volume ( $\mu\text{m}^3$ )                        | 663.73          | 513.32                  | 873.25         | 178.13                  | $p > 0.05$       |
| Rhizoidal Growth Unit ( $\mu\text{m}$ )           | 12.41           | 2.78                    | 18.35          | 2.05                    | $p < 0.001$      |
| Cover Area ( $\mu\text{m}^2$ )                    | 20192.72        | 7376.37                 | 27145.56       | 3479.91                 | $p < 0.05$       |
| Mean Bifurcation Angle ( $^\circ$ )               | 82.90           | 3.27                    | 81.86          | 6.59                    | $p > 0.05$       |
| Partition Asymmetry                               | 0.56            | 0.06                    | 0.64           | 0.07                    | $p < 0.05$       |
| Max Euclidean Distance ( $\mu\text{m}$ )          | 33.95           | 16.23                   | 48.33          | 9.11                    | $p > 0.05$       |
| Max Path Distance ( $\mu\text{m}$ )               | 44.62           | 17.45                   | 64.48          | 11.60                   | $p < 0.05$       |
| <b>10 <math>\mu\text{M}</math> Cytochalasin B</b> | <b>Poisoned</b> | <b><math>\pm</math></b> | <b>Control</b> | <b><math>\pm</math></b> |                  |
| <b>Morphometric Feature</b>                       | <b>Cells</b>    | <b>Standard</b>         | <b>Cells</b>   | <b>Standard</b>         | <b>t-test p-</b> |
|   | <b>(Mean)</b>   | <b>Deviation</b>        | <b>(Mean)</b>  | <b>Deviation</b>        | <b>value</b>     |
| Thallus Diameter ( $\mu\text{m}^2$ )              | 104.17          | 23.54                   | 124.72         | 13.06                   | $p < 0.05$       |
| Number of Bifurcations                            | 10.78           | 1.79                    | 16.33          | 3.43                    | $p < 0.01$       |
| Number of Tips                                    | 14.00           | 2.40                    | 19.22          | 2.44                    | $p < 0.001$      |
| Width ( $\mu\text{m}$ )                           | 145.38          | 12.72                   | 179.84         | 22.04                   | $p < 0.01$       |
| Height ( $\mu\text{m}$ )                          | 103.63          | 28.11                   | 139.30         | 16.38                   | $p < 0.01$       |
| Depth ( $\mu\text{m}$ )                           | 8.70            | 2.56                    | 8.92           | 2.64                    | $p > 0.05$       |
| Total Length ( $\mu\text{m}$ )                    | 119.58          | 61.95                   | 319.61         | 57.12                   | $p < 0.001$      |
| Surface Area ( $\mu\text{m}^2$ )                  | 489.73          | 237.80                  | 1099.97        | 250.29                  | $p < 0.001$      |
| Volume ( $\mu\text{m}^3$ )                        | 259.75          | 97.96                   | 449.04         | 115.66                  | $p < 0.01$       |
| Rhizoidal Growth Unit ( $\mu\text{m}$ )           | 8.68            | 4.52                    | 16.62          | 2.06                    | $p < 0.01$       |
| Cover Area ( $\mu\text{m}^2$ )                    | 15140.54        | 4661.50                 | 25114.02       | 4842.67                 | $p < 0.001$      |
| Mean Bifurcation Angle ( $^\circ$ )               | 90.58           | 5.79                    | 90.28          | 7.59                    | $p > 0.05$       |
| Partition Asymmetry                               | 0.49            | 0.09                    | 0.62           | 0.08                    | $p < 0.01$       |
| Max Euclidean Distance ( $\mu\text{m}$ )          | 18.43           | 9.74                    | 34.84          | 10.48                   | $p < 0.01$       |
| Max Path Distance ( $\mu\text{m}$ )               | 22.91           | 12.39                   | 52.32          | 19.61                   | $p < 0.01$       |



Supplementary Table 3

| <b>(1 h)</b><br><b>Morphometric Feature</b> | <b>Carbon Replete (Mean)</b> | <b>± Standard Deviation</b> | <b>Carbon Deplete (Mean)</b> | <b>± Standard Deviation</b> | <b>t-test p-value</b> |
|---|------------------------------|-----------------------------|------------------------------|-----------------------------|-----------------------|
| Thallus Diameter ( $\mu\text{m}^2$ )        | 65.33                        | 10.96                       | 51.85                        | 11.85                       | $p < 0.01$            |
| Number of Bifurcations                      | 4.33                         | 1.58                        | 3.63                         | 2.70                        | $p > 0.05$            |
| Number of Tips                              | 5.78                         | 1.30                        | 4.75                         | 2.60                        | $p > 0.05$            |
| Width ( $\mu\text{m}$ )                     | 47.59                        | 7.42                        | 42.38                        | 22.60                       | $p > 0.05$            |
| Height ( $\mu\text{m}$ )                    | 49.04                        | 12.71                       | 45.21                        | 20.65                       | $p > 0.05$            |
| Depth ( $\mu\text{m}$ )                     | 7.58                         | 2.60                        | 6.74                         | 1.68                        | $p > 0.05$            |
| Total Length ( $\mu\text{m}$ )              | 75.54                        | 16.57                       | 74.47                        | 55.59                       | $p > 0.05$            |
| Surface Area ( $\mu\text{m}^2$ )            | 207.65                       | 36.34                       | 173.69                       | 205.38                      | $p > 0.05$            |
| Volume ( $\mu\text{m}^3$ )                  | 98.70                        | 22.65                       | 70.36                        | 70.72                       | $p < 0.001$           |
| Rhizoidal Growth Unit ( $\mu\text{m}$ )     | 13.19                        | 1.53                        | 15.82                        | 2.75                        | $p > 0.05$            |
| Cover Area ( $\mu\text{m}^2$ )              | 2400.60                      | 934.82                      | 1959.75                      | 2892.47                     | $p > 0.05$            |
| Mean Bifurcation Angle ( $^\circ$ )         | 93.94                        | 16.81                       | 92.24                        | 16.11                       | $p > 0.05$            |
| Partition Asymmetry                         | 0.50                         | 0.13                        | 0.54                         | 0.17                        | $p > 0.05$            |
| Max Euclidean Distance ( $\mu\text{m}$ )    | 11.26                        | 4.81                        | 13.08                        | 11.37                       | $p > 0.05$            |
| Max Path Distance ( $\mu\text{m}$ )         | 13.67                        | 5.78                        | 16.05                        | 12.60                       | $p > 0.05$            |
| <b>(4 h)</b><br><b>Morphometric Feature</b> | <b>Carbon Replete (Mean)</b> | <b>± Standard Deviation</b> | <b>Carbon Deplete (Mean)</b> | <b>± Standard Deviation</b> | <b>t-test p-value</b> |
| Thallus Diameter ( $\mu\text{m}^2$ )        | 103.87                       | 16.89                       | 70.28                        | 10.53                       | $p < 0.001$           |
| Number of Bifurcations                      | 14.38                        | 4.47                        | 10.44                        | 2.88                        | $p > 0.05$            |
| Number of Tips                              | 16.25                        | 4.33                        | 12.00                        | 2.74                        | $p < 0.05$            |
| Width ( $\mu\text{m}$ )                     | 102.31                       | 17.57                       | 142.60                       | 20.37                       | $p < 0.001$           |
| Height ( $\mu\text{m}$ )                    | 103.86                       | 22.07                       | 152.28                       | 40.59                       | $p < 0.01$            |
| Depth ( $\mu\text{m}$ )                     | 9.35                         | 1.63                        | 7.23                         | 1.68                        | $p < 0.05$            |
| Total Length ( $\mu\text{m}$ )              | 297.44                       | 91.96                       | 400.84                       | 41.77                       | $p < 0.05$            |
| Surface Area ( $\mu\text{m}^2$ )            | 1052.25                      | 355.81                      | 1353.25                      | 399.14                      | $p > 0.05$            |
| Volume ( $\mu\text{m}^3$ )                  | 413.31                       | 174.59                      | 440.55                       | 231.56                      | $p > 0.05$            |
| Rhizoidal Growth Unit ( $\mu\text{m}$ )     | 18.23                        | 2.12                        | 35.06                        | 9.50                        | $p < 0.001$           |
| Cover Area ( $\mu\text{m}^2$ )              | 10840.47                     | 3982.10                     | 22043.11                     | 7629.16                     | $p < 0.01$            |
| Mean Bifurcation Angle ( $^\circ$ )         | 79.35                        | 8.36                        | 86.91                        | 7.40                        | $p > 0.05$            |
| Partition Asymmetry                         | 0.60                         | 0.11                        | 0.58                         | 0.09                        | $p > 0.05$            |
| Max Euclidean Distance ( $\mu\text{m}$ )    | 41.41                        | 10.76                       | 75.16                        | 22.69                       | $p < 0.01$            |
| Max Path Distance ( $\mu\text{m}$ )         | 47.53                        | 10.83                       | 91.44                        | 23.97                       | $p < 0.001$           |
| <b>(7 h)</b><br><b>Morphometric Feature</b> | <b>Carbon Replete (Mean)</b> | <b>± Standard Deviation</b> | <b>Carbon Deplete (Mean)</b> | <b>± Standard Deviation</b> | <b>t-test p-value</b> |

|  |                              |  |                              |  |                       |
|--|------------------------------|--|------------------------------|--|-----------------------|
| Thallus Diameter ( $\mu\text{m}^2$ )     | 179.38                       | 28.07                                      | 85.36                        | 85.36                                      | $p < 0.001$           |
| Number of Bifurcations                   | 25.67                        | 6.08                                       | 25.56                        | 25.56                                      | $p > 0.05$            |
| Number of Tips                           | 28.11                        | 6.33                                       | 26.89                        | 26.89                                      | $p > 0.05$            |
| Width ( $\mu\text{m}$ )                  | 173.98                       | 19.14                                      | 185.34                       | 185.34                                     | $p > 0.05$            |
| Height ( $\mu\text{m}$ )                 | 166.68                       | 26.11                                      | 215.32                       | 215.32                                     | $p < 0.05$            |
| Depth ( $\mu\text{m}$ )                  | 10.88                        | 3.14                                       | 10.85                        | 10.85                                      | $p > 0.05$            |
| Total Length ( $\mu\text{m}$ )           | 635.08                       | 135.09                                     | 800.14                       | 800.14                                     | $p < 0.05$            |
| Surface Area ( $\mu\text{m}^2$ )         | 2394.43                      | 484.77                                     | 2914.51                      | 2914.51                                    | $p > 0.05$            |
| Volume ( $\mu\text{m}^3$ )               | 982.62                       | 190.12                                     | 946.72                       | 946.72                                     | $p > 0.05$            |
| Rhizoidal Growth Unit ( $\mu\text{m}$ )  | 23.00                        | 4.75                                       | 31.23                        | 31.23                                      | $p < 0.05$            |
| Cover Area ( $\mu\text{m}^2$ )           | 29227.45                     | 6934.82                                    | 39176.52                     | 39176.52                                   | $p < 0.05$            |
| Mean Bifurcation Angle ( $^\circ$ )      | 82.19                        | 6.23                                       | 88.03                        | 88.03                                      | $p < 0.05$            |
| Partition Asymmetry                      | 0.63                         | 0.07                                       | 0.65                         | 0.65                                       | $p > 0.05$            |
| Max Euclidean Distance ( $\mu\text{m}$ ) | 62.15                        | 7.66                                       | 120.92                       | 120.92                                     | $p < 0.01$            |
| Max Path Distance ( $\mu\text{m}$ )      | 75.05                        | 5.18                                       | 156.50                       | 156.50                                     | $p < 0.001$           |
| <b>(24 h)</b>                            |                              |  |                              |  |                       |
| <b>Morphometric Feature</b>              | <b>Carbon Replete (Mean)</b> | <b><math>\pm</math> Standard Deviation</b> | <b>Carbon Deplete (Mean)</b> | <b><math>\pm</math> Standard Deviation</b> | <b>t-test p-value</b> |
| Thallus Diameter ( $\mu\text{m}^2$ )     | 2038.41                      | 336.41                                     | 180.49                       | 24.79                                      | $p < 0.01$            |
| Number of Bifurcations                   | 365.75                       | 80.22                                      | 88.00                        | 24.42                                      | $p < 0.01$            |
| Number of Tips                           | 433.25                       | 106.58                                     | 90.63                        | 23.74                                      | $p < 0.01$            |
| Width ( $\mu\text{m}$ )                  | 402.03                       | 28.77                                      | 364.64                       | 48.94                                      | $p < 0.05$            |
| Height ( $\mu\text{m}$ )                 | 401.90                       | 15.90                                      | 393.74                       | 19.71                                      | $p > 0.05$            |
| Depth ( $\mu\text{m}$ )                  | 25.14                        | 5.19                                       | 9.69                         | 2.75                                       | $p < 0.01$            |
| Total Length ( $\mu\text{m}$ )           | 9918.81                      | 2094.98                                    | 3015.64                      | 815.10                                     | $p < 0.01$            |
| Surface Area ( $\mu\text{m}^2$ )         | 43028.44                     | 9579.73                                    | 12093.19                     | 3594.02                                    | $p < 0.01$            |
| Volume ( $\mu\text{m}^3$ )               | 28425.62                     | 4653.46                                    | 4245.75                      | 1349.18                                    | $p < 0.01$            |
| Rhizoidal Growth Unit ( $\mu\text{m}$ )  | 23.16                        | 1.92                                       | 33.23                        | 2.53                                       | $p < 0.001$           |
| Cover Area ( $\mu\text{m}^2$ )           | 161828.23                    | 16638.78                                   | 143817.79                    | 22032.07                                   | $p > 0.05$            |
| Mean Bifurcation Angle ( $^\circ$ )      | 68.06                        | 3.21                                       | 81.69                        | 2.63                                       | $p < 0.01$            |
| Partition Asymmetry                      | 0.64                         | 0.00                                       | 0.67                         | 0.06                                       | $p > 0.05$            |
| Max Euclidean Distance ( $\mu\text{m}$ ) | 206.91                       | 18.27                                      | 181.53                       | 34.94                                      | $p > 0.05$            |
| Max Path Distance ( $\mu\text{m}$ )      | 256.90                       | 24.26                                      | 235.21                       | 82.52                                      | $p > 0.05$            |

Supplementary Table 4

| <b>Particulate Carbon<br/>Morphometric Feature</b> | <b>(1 h)<br/>(Mean)</b> | <b>±<br/>Standard<br/>Deviation</b> | <b>(4 h)<br/>(Mean)</b> | <b>±<br/>Standard<br/>Deviation</b> | <b>(7 h)<br/>(Mean)</b> | <b>±<br/>Standard<br/>Deviation</b> | <b>(24 h)<br/>(Mean)</b> | <b>±<br/>Standard<br/>Deviation</b> |
|--|-------------------------|-------------------------------------|-------------------------|-------------------------------------|-------------------------|-------------------------------------|--------------------------|-------------------------------------|
| Thallus Diameter ( $\mu\text{m}^2$ )               | 71.38                   | 12.81                               | 83.29                   | 9.78                                | 91.89                   | 16.18                               | 269.71                   | 55.76                               |
| Number of Bifurcations                             | 2.22                    | 1.30                                | 8.89                    | 4.70                                | 10.75                   | 4.83                                | 112.75                   | 62.47                               |
| Number of Tips                                     | 3.22                    | 1.30                                | 10.89                   | 5.49                                | 13.50                   | 6.07                                | 143.50                   | 91.81                               |
| Width ( $\mu\text{m}$ )                            | 131.18                  | 14.57                               | 152.85                  | 30.43                               | 153.14                  | 17.21                               | 171.85                   | 15.96                               |
| Height ( $\mu\text{m}$ )                           | 97.68                   | 23.73                               | 105.45                  | 22.29                               | 121.57                  | 33.43                               | 145.96                   | 28.79                               |
| Depth ( $\mu\text{m}$ )                            | 6.92                    | 2.26                                | 32.81                   | 15.63                               | 42.38                   | 9.70                                | 58.99                    | 10.02                               |
| Total Length ( $\mu\text{m}$ )                     | 32.95                   | 16.05                               | 191.55                  | 73.31                               | 324.11                  | 108.77                              | 2160.80                  | 722.46                              |
| Surface Area ( $\mu\text{m}^2$ )                   | 151.11                  | 48.92                               | 715.97                  | 237.15                              | 1164.11                 | 457.21                              | 7260.26                  | 3195.89                             |
| Volume ( $\mu\text{m}^3$ )                         | 104.61                  | 26.55                               | 291.69                  | 96.99                               | 422.49                  | 177.54                              | 2740.66                  | 1364.26                             |
| Rhizoidal Growth Unit ( $\mu\text{m}$ )            | 10.50                   | 4.15                                | 18.97                   | 5.76                                | 25.68                   | 6.64                                | 17.54                    | 5.72                                |
| Cover Area ( $\mu\text{m}^2$ )                     | 12718.87                | 2934.84                             | 15959.67                | 4130.87                             | 18483.84                | 4996.53                             | 24937.91                 | 4319.79                             |
| Mean Bifurcation Angle ( $^\circ$ )                | 94.20                   | 18.51                               | 81.76                   | 12.22                               | 92.12                   | 9.37                                | 82.45                    | 1.73                                |
| Partition Asymmetry                                | 0.37                    | 0.28                                | 0.40                    | 0.19                                | 0.56                    | 0.07                                | 0.58                     | 0.12                                |
| Max Euclidean Distance<br>( $\mu\text{m}$ )        | 10.43                   | 5.91                                | 52.95                   | 31.98                               | 43.05                   | 17.77                               | 41.48                    | 15.56                               |
| Max Path Distance ( $\mu\text{m}$ )                | 12.63                   | 7.17                                | 88.61                   | 61.80                               | 66.92                   | 21.46                               | 63.91                    | 15.28                               |

Supplementary Table 5

| <b>Rhizoid Differentiation Morphometric Feature</b> | <b>Particle Associated (Mean)</b> | <b>± Standard Deviation</b> | <b>Not Particle Associated (Mean)</b> | <b>± Standard Deviation</b> | <b>t-test p-value</b> |
|---|-----------------------------------|-----------------------------|---------------------------------------|-----------------------------|-----------------------|
| Number of Bifurcations                              | 24.63                             | 11.33                       | 28.50                                 | 8.65                        | $p > 0.05$            |
| Number of Tips                                      | 30.50                             | 12.75                       | 30.25                                 | 8.43                        | $p > 0.05$            |
| Width ( $\mu\text{m}$ )                             | 150.84                            | 22.60                       | 217.94                                | 10.43                       | $p < 0.001$           |
| Height ( $\mu\text{m}$ )                            | 146.25                            | 31.11                       | 201.50                                | 29.49                       | $p < 0.001$           |
| Depth ( $\mu\text{m}$ )                             | 33.32                             | 6.52                        | 9.49                                  | 5.17                        | $p < 0.001$           |
| Total Length ( $\mu\text{m}$ )                      | 465.18                            | 167.59                      | 1090.68                               | 310.27                      | $p < 0.01$            |
| Surface Area ( $\mu\text{m}^2$ )                    | 1415.67                           | 623.56                      | 3913.74                               | 1420.74                     | $p < 0.01$            |
| Volume ( $\mu\text{m}^3$ )                          | 406.93                            | 236.86                      | 1291.92                               | 595.80                      | $p < 0.001$           |
| Rhizoidal Growth Unit ( $\mu\text{m}$ )             | 15.88                             | 4.42                        | 36.16                                 | 4.44                        | $p < 0.001$           |
| Cover Area ( $\mu\text{m}^2$ )                      | 22093.22                          | 6323.01                     | 43929.59                              | 6729.19                     | $p < 0.001$           |
| Mean Bifurcation Angle ( $^\circ$ )                 | 85.71                             | 9.99                        | 92.76                                 | 7.28                        | $p < 0.001$           |
| Partition Asymmetry                                 | 0.54                              | 0.11                        | 0.53                                  | 0.15                        | $p > 0.05$            |
| Max Euclidean Distance ( $\mu\text{m}$ )            | 32.80                             | 11.82                       | 127.76                                | 27.94                       | $p < 0.001$           |
| Max Path Distance ( $\mu\text{m}$ )                 | 85.76                             | 41.84                       | 171.28                                | 57.36                       | $p < 0.05$            |